Evaluation of MIMO Stationarity

OMAR ALDAYEL

KTH Electrical Engineering

Master's Degree Project
Stockholm, Sweden

XR–EE–SB 2011:005

Royal institute of Technology KTH

Evaluation of MIMO Non-Stationarity

Omar Aldayel

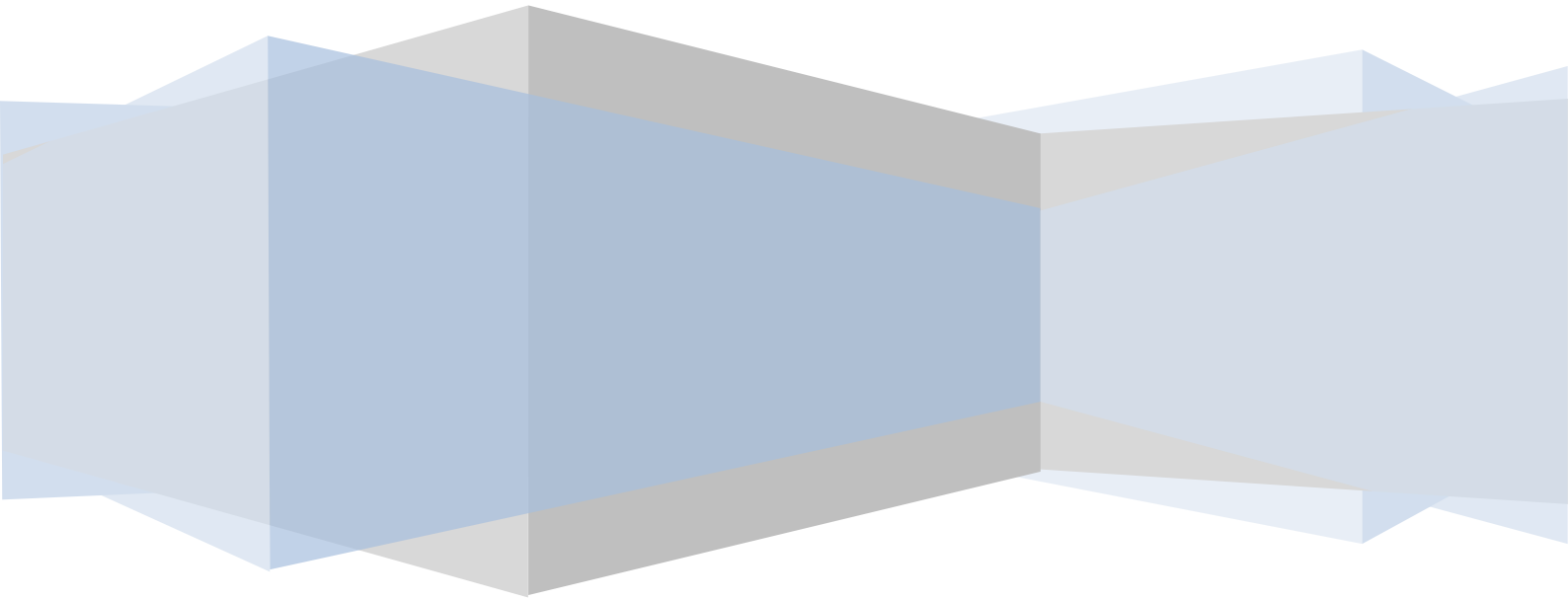

Contents

Abstract

The transmission performance of MIMO systems can be highly improved under stationary channel conditions where the channel statistics are constant. Unfortunately, mobile radio channels are not stationary all the time. Instead, they are stationary for finite time durations, so-called the stationarity regions. If these stationarity regions are relatively large, then the channel statistics can be utilized during each stationarity region to enhance the transmission performance. Therefore, it is necessary to examine the stationarity of mobile channels and characterize the stationarity regions.

This thesis investigates the non-stationarity of measured MIMO channels and proposes some stationarity metrics to measure it. These metrics are: the CMD proposed by [**1**], NCMD and DES. Each one of the metrics is relevant to different types of transmission schemes and scenarios. The CMD may not be accurate for some transmission scenarios; therefore, the NCMD, which is a normalized version of CMD, is proposed. Theoretically, the NCMD can be at most 100% higher than the CMD for a 4x4 MIMO system. For beamforming scenario, the DES metric can be used to describe the non-stationarity of few eigenvectors taken from the channel variance. Under the measured MIMO channels, it was found that the CMD overestimates the stationarity regions compared to the NCMD and DES metrics particularly under the NLOS routes.

Acknowledgments

I would like to express my thanks and gratitude to my advisor, Mats Bengtsson for giving me the opportunity to work on this thesis with the Signal Processing Laboratory at KTH. I would like also to thank him for his endless help, advice and patience.

I would like also to thank my opponent, Ali Al-Enezi for his opinions, support and contributions.

Very special thanks to my family for their love and nonstop support during my studies.

Acronyms

CCF	Channel Correlation Function
CMD	Correlation Matrix Distance
DES	Distance between Equidimensional Subspaces
DU	Doubly Underspread
LCF	Local Correlation Function
LOS	Line Of Sight
LTE	Long term Evolution
LTV	Linear Time Variant
MIMO	Multiple Input Multiple Output
NCMD	Normalized Correlation Matrix Distance
NLOS	Non Line Of Sight
OFDM	Orthogonal Frequency Division Multiplexing
QWSSUS	Quasi Wide Sense Stationary Uncorrelated Scattering
SISO	Single Output Single Input
SVD	Singular Value Decomposition
US	Uncorrelated Scattering
WSS	Wide Sense Stationary
WSSUS	Wide Sense Stationary Uncorrelated Scattering

Notation

$\mathbf{A}$	Boldface and upper case characters for matrices
$\mathbf{a}$	Boldface and lower case characters for vectors
$(\cdot)^T$	Transpose of a matrix
$(\cdot)^*$	Conjugate of a scalar or matrix
$(\cdot)^H$	Hermitian of a matrix
$\|\cdot\|_F$	Frobenius norm of a matrix
$\|\cdot\|_2$	Norm two of a vector
$\mathrm{vec}\{\cdot\}$	Vectorization of a matrix
$\otimes$	Kronecker product
$E[\cdot]$	Expected value of a random variable or a stochastic process

Chapter 1
Introduction

Since the invention of Multiple-Input Multiple-Output (MIMO) technology from more than a decade ago, a lot of wireless transmission schemes have been developed to improve the performance and reliability of MIMO systems. The main reason behind these large interests is to achieve higher data rates or to increase the system reliability with the same amount of power and bandwidth compared to typical Single-Input Single-Output (SISO) systems as theoretical analysis of MIMO communications promises. However, according to [**2**] a large number of the developed MIMO communication transmission schemes have not been examined under real MIMO channel conditions so far.

The optimum transmission performance of MIMO channels can be achieved if the instantaneous channel gains are known at both the transmitter and receiver. For mobile channels, where the channel gains are fast varying with time, the instantaneous channel knowledge cannot be obtained at the transmitter. Therefore, the channel statistics are used instead of the instantaneous values. In this case, the transmission performance of the channel will be slightly lower than the optimum, in general, and close to the optimum for some transmission schemes and scenarios[**3**].

Consequently, some of the advanced MIMO transmission schemes are based on the channel statistics knowledge. However, these types of transmission schemes cannot be utilized under non-stationary channel conditions where the MIMO channel statistics change very quickly, since the receiver will not be able to feed back the channel statistical information to the transmitter. On the other hand, if the channel statistics are constant (quasi-stationary) during some relatively large stationarity region, then these schemes can be applied within this stationarity region. Therefore, it is very important to estimate the stationarity regions of real MIMO channels to see whether these types of transmission schemes are applicable or not.

According to [**1**], unlike real Single-Input-Single-Output (SISO) channels, real MIMO channels depends on the spatial structure of the antennas (angles of the transmit and receive antennas) and multipath components more strongly. Therefore, the stationarity of such channels depend mainly on the spatial structure in addition to time and frequency.

In KTH Signal Processing Lab, we have a large data set of real measured MIMO channels. We would like to examine and evaluate the stationarity of these channels and try to characterize and evaluate the stationarity regions within it.

1.1 Previous work

The non-stationarity of SISO channels has been investigated by Matz [**4**]. There, a Channel Correlation Function (CCF) was introduced to estimate the stationarity region of SISO channels. For the SIMO channels, a stationarity measure relevant to the beamforming scenario has been introduced by [**5**] so-called F-eigen ratio. F-eigen ratio measures the similarity between the out-dated and new channel covariance matrices with respect to the largest F eigenmodes. The non-stationarity of MIMO channels have been investigated by Herdin in his thesis [**1**]. There, he provides a function that measures the dissimilarity of two different matrices called the Correlation Matrix Distance (CMD). However, CMD may not be very precise in evaluating the non-stationarity of MIMO channels if the two matrices are high rank (i.e. have more linearly independent columns). In this case, the CMD can be very small even if the two matrices are different.

1.2 Objective

We will try to apply different methods to evaluate the non-stationarity of the measured MIMO channels versus the separation in a specific domain (time, frequency or space). In general, these methods measure the distance (dissimilarity) between two matrices and produce a single value that ranges from zero to one. For instance, the CMD calculates the distance between two correlation matrices $\mathbf{R}_1$ and $\mathbf{R}_2$ by using the inner product as:

$$d_{CMD}(\mathbf{R_1}, \mathbf{R_2}) = 1 - \frac{\mathrm{tr}\{\mathbf{R_1}\mathbf{R_2}\}}{\|\mathbf{R_1}\|_F \|\mathbf{R_2}\|_F}$$

Where $\|\cdot\|_F$ is the Frobenius norm and $\mathrm{tr}\{\cdot\}$ is the matrix trace. Matrix distance measures can achieve a maximum value of 1 indicating that the two matrices are orthogonal, and a minimum value of 0 indicating that the two matrices are equal except for a scaling factor. We will try to find different methods to measure the distance between two matrices and then we will use them to evaluate the non-stationarity region of the measured MIMO channels.

Chapter 2

Background

2.1 Classifications of Radio Channels

In this section, we will discuss some basic classifications of mobile radio channels for typical Single-Input-Single-Output (SISO) systems.

Mobile radio channels are time and frequency varying due to movements in the communication medium and multipath components. Therefore, a mobile radio channel can be seen as linear time varying (LTV) filter $h(t,\tau)$. If $s(t)$ is the transmitted signal through $h(t,\tau)$ then the received signal is given as:

$$r(t) = \int_{\tau=-\infty}^{\infty} h(t,\tau)\, s(t-\tau)\, d\tau$$

Alternatively, the channel can be written as a time and frequency varying function $H(t,f)$ by using Fourier transform with respect to τ as:

$$H(t,f) = \int_{\tau=-\infty}^{\infty} h(t,\tau)\, e^{-j2\pi f\tau}\, d\tau$$

2.1.1 Coherence Time and Frequency

The coherence time T_c of $h(t,f)$ is defined as the time duration at which the channel can be assumed constant over time. If we transmit two pulses through the channel at different time instances t_1 and t_2 then:

$$H(t_1,f) \approx H(t_2,f), \quad \text{for} \quad |t_1 - t_2| < T_c$$

Similarly, the coherence bandwidth B_c of $H(t,f)$ is defined as the frequency band at which the channel can be assumed constant over frequency. If we transmit two sinusoid signals through the channel at different frequencies f_1 and f_2 then:

$$H(t,f_1) \approx H(t,f_2), \quad \text{for} \quad |f_1 - f_2| < B_c$$

2.1.2 Fading Channels

Time-variant channels are classified to different categories based on the coherence time and coherence bandwidth. If the transmission through the time-variant channel is made over the symbol duration T and bandwidth B, then the channel is said to be:

- **Slow Fading Channel:** If the coherence time is much larger than the symbol duration ($T_c \gg T$). Here, the channel can be assumed time invariant:

$$h(t,\tau) \approx h(\tau)$$

and the received signal through this channel is:

$$r(t) = \int_{\tau=-\infty}^{\infty} h(\tau)\, s(t-\tau)\, d\tau$$

- **Frequency Flat Channel:** If the coherence bandwidth is much larger than the system bandwidth ($B_c \gg B$). Here, the channel can be assumed frequency invariant :

$$H(t,f) \approx H(t)$$

and the received signal through this channel is:

$$r(t) = h(t)\, s(t)$$

- **Fast Fading Channel (time selective):** If the coherence time is smaller than or equal to the symbol duration ($T_c \leq T$). In this case, the channel cannot be assumed time invariant.
- **Frequency Selective Channel:** If the coherence bandwidth is smaller than or equal to the system bandwidth ($B_c \leq B$). In this case, the channel cannot be assumed frequency invariant.

2.1.3 OFDM

Under frequency selective channels, Orthogonal Frequency Division Multiplexing (OFDM) can be used to overcome frequency fading. In OFDM, the channel bandwidth is divided to orthogonal subbands and the transmission is made through each subband with independent signal. If each subband is smaller than the coherence bandwidth, then the signal in one OFDM subband exhibits flat fading. The OFDM subband signal is given as:

$$s_k(t) = A_k \cos(2\pi f_k t)$$

Where T is the symbol duration. If the fading channel is given by $H(t,f)$, then the received signal is:

$$r(t) = H(t,f_k)s_k(t) = H_k(t)s_k(t) \qquad (1)$$

where $H_k(t)$ is a time varying and frequency flat channel.

2.1.4 Stochastic Channels

If the channel in equation (1) is a time selective channel, then $H_k(t)$ changes in unpredictable manner during the symbol time T and the value of $H_k(t)$ is unknown. Therefore, it is reasonable to model $H_k(t)$ as a stochastic process. If the channel is stationary stochastic process, the channel statistics, like the mean and variance, are not time varying and can be estimated at the receiver side and then feed back to the transmitter. For MIMO channels, the channel statistics knowledge increases the performance of the MIMO communication systems compared to the performance when no channel knowledge is available. In the Sec. 2.4, we will discuss the stationarity of radio channels in more details.

2.2 MIMO Communication Systems

Communication systems can have different setups regarding the number of antennas at the transmit and receive sides. Typically, communication systems use one transmit antenna and one receive antenna, so-called single-input single-output (SISO) systems. On the other hand, multiple-input multiple-output (MIMO) communication systems use multiple antennas at both the transmitter and receiver as shown in Figure 1. MIMO transmit antennas can send different signals at the same time and frequency. At the receiver side, each antenna receives multiple signals from all the transmit antennas. Thus, MIMO transmit and receive signals are represented as vectors while the MIMO channel function is represented as a matrix.

In the next section, we will give a brief overview of the MIMO system described in [**6**] and [**3**].

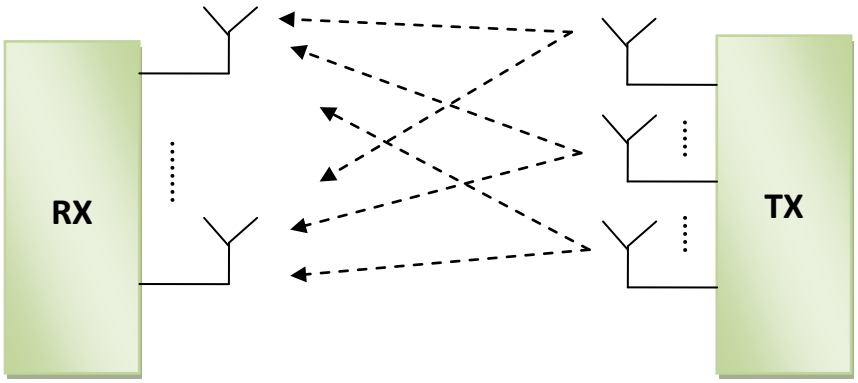

Figure 1: MIMO system setup with multiple antennas at transmit and receive sides.

2.2.1 MIMO System Model

Consider a MIMO system with n_T transmit antennas and n_R receive antennas. The time-invariant and frequency flat MIMO channel is given as $n_R \times n_T$ matrix:

$$\mathbf{H} = \begin{bmatrix} h_{11} & h_{12} & \cdots & h_{1n_T} \\ h_{21} & h_{22} & & h_{2n_T} \\ \vdots & \vdots & \ddots & \vdots \\ h_{n_R1} & h_{n_R2} & \cdots & h_{n_Rn_T} \end{bmatrix} \quad (2)$$

where h_{ij} is the channel gain of the path between the transmit antenna number j and the receive antenna number i. If $\mathbf{s}(t) = [s_1(t)\ s_2(t)\ \ldots\ s_{n_T}(t)]^T$ is the transmitted signal vector through the above MIMO channel matrix then the received signal vector $\mathbf{r}(t) = [r_1(t)\ r_2(t)\ \cdots\ r_{n_R}(t)]$ is given as:

$$\mathbf{r}(t) = \mathbf{H}\,\mathbf{s}(t) + \mathbf{n}(t) \quad (3)$$

where $\mathbf{n}(t) = [n_1(t)\ n_2(t)\ \ldots\ n_{n_R}(t)]^T$ is the noise vector. Time invariant and frequency flat MIMO channel has a favorable property. Since the channel gains are constant, they can be estimated at the receiver by using training sequence and then forwarded to the transmitter. Thus, the transmitter can allocate power through the strongest channel paths, as will be discussed in the next section.

2.2.2 Constant MIMO Channel Capacity

The MIMO channel capacity C (the maximum mutual information between the input and the output) over a time invariant and frequency flat MIMO channel $\mathbf{H}$ is given by:

$$C = \max_{\|\mathbf{Q}\|=P} \log_2 \det(\mathbf{I}_{n_R} + \frac{1}{N_0}\mathbf{H}\mathbf{Q}\mathbf{H}^H)$$

where $\mathbf{Q}$ is the input covariance matrix, P is the total transmit power and N_0 is the noise power. The optimal input covariance matrix $\mathbf{Q}$ can be exploited if the channel is completely known at both the transmitter and the receiver. To illustration this, we need to decompose the channel matrix $\mathbf{H}$ using Singular Value Decomposition (SVD) as follows:

$$\mathbf{H} = \mathbf{U}\mathbf{\Sigma}\mathbf{V}^H$$

where $\mathbf{U}$ and $\mathbf{V}$ are, respectively, $n_R \times n_R$ and $n_T \times n_T$ unitary matrices and $\mathbf{\Sigma}$ is $n_R \times n_T$ diagonal matrix contains the singular values of $\mathbf{H}$ sorted from maximum to minimum as $\sigma_1 \geq \sigma_2 \geq \cdots \geq \sigma_{\min(n_R,n_T)}$.

In general, parallel data streams can be utilized if the MIMO channel $\mathbf{H}$ is known at the transmitter and receiver. For instance, if $\tilde{\mathbf{s}}(t)$ is the data vector at the transmitter, then we can set the transmitted vector $\mathbf{s}(t)$ as:

$$\mathbf{s}(t) = \mathbf{V}\,\tilde{\mathbf{s}}(t)$$

Consequently, we will have the following received vector $\mathbf{r}(t)$:

$$\begin{aligned}\mathbf{r}(t) &= \mathbf{H}\,\mathbf{s}(t) + \mathbf{n}(t)\\ &= (\mathbf{U}\boldsymbol{\Sigma}\mathbf{V}^H)\left(\mathbf{V}\,\tilde{\mathbf{s}}(t)\right) + \mathbf{n}(t)\\ &= \mathbf{U}\boldsymbol{\Sigma}\,\tilde{\mathbf{s}}(t) + \mathbf{n}(t)\end{aligned}$$

At the receiver, we can extract the received data vector $\tilde{\mathbf{r}}(t)$ as:

$$\begin{aligned}\tilde{\mathbf{r}}(t) &= \mathbf{U}^H\,\mathbf{r}(t)\\ &= \mathbf{U}^H\,\mathbf{U}\boldsymbol{\Sigma}\,\tilde{\mathbf{s}}(t) + \mathbf{U}^H\mathbf{n}(t)\\ &= \boldsymbol{\Sigma}\tilde{\mathbf{s}}(t) + \tilde{\mathbf{n}}(t)\end{aligned}$$

Alternatively, $\tilde{\mathbf{r}}(t)$ can be written as:

$$\tilde{r}_i(t) = \sigma_i\,\tilde{s}_i(t) + \tilde{n}_i(t)$$

In this case, the optimal input covariance matrix $\mathbf{Q}$ is given by:

$$\mathbf{Q} = \mathbf{V}\mathbf{P}\mathbf{V}^H \qquad (4)$$

where $\mathbf{P} = \mathrm{diag}(P_1, P_2, \ldots, P_{n_T})$ is a $n_T \times n_T$ power matrix and P_i is the power of $\tilde{s}_i(t)$ allocated as:

$$P_i = \left(\mu - \frac{1}{\sigma_i^2}\right)^+ \qquad (5)$$

where x^+ indicates maximum$(x, 0)$ and μ is selected such that $\sum_{i=1}^{n_T} P_i = P$. The power allocation in equation (5) will allocate more power in the largest singular values of $\mathbf{H}$ and no power will be allocated for low singular values.

Nevertheless, if the channel information is unknown at the transmitter, then the power allocation will be uniformly distributed over the transmit antennas i.e. $P_i = P/n_T$ and $\mathbf{Q} = P/n_T\,\mathbf{I}_{n_T}$. In this case, the channel mutual information will be lower than the channel capacity.

2.3 Time-Variant MIMO Channels

The MIMO channel capacity can be achieved if the MIMO channel gains are known at both the transmitter and receiver. Unfortunately, mobile MIMO channels are time and frequency selective. In general, the MIMO channel impulse response is given as a linear time varying filter:

$$\mathbf{H}(t,\tau) = \begin{bmatrix} h_{11}(t,\tau) & h_{12}(t,\tau) & \cdots & h_{1n_T}(t,\tau) \\ h_{21}(t,\tau) & h_{22}(t,\tau) & & h_{2n_T}(t,\tau) \\ \vdots & \vdots & \ddots & \vdots \\ h_{n_R1}(t,\tau) & h_{n_R2}(t,\tau) & \cdots & h_{n_Rn_T}(t,\tau) \end{bmatrix} \quad (6)$$

If $\mathbf{s}(t)$ is the transmitted signal through $\mathbf{H}(t,\tau)$ then the received signal can be written as:

$$\mathbf{r}(t) = \int_{\tau=-\infty}^{\infty} \mathbf{H}(t,\tau)\, \mathbf{s}(t-\tau)\, d\tau + \mathbf{n}(t) \quad (7)$$

The frequency spectrum of the channel is given by the Fourier transform of $\mathbf{H}(t,\tau)$ with respect to τ:

$$\mathbf{H}(t,f) = \int_{\tau=-\infty}^{\infty} \mathbf{H}(t,\tau)\, e^{-j2\pi f\tau}\, d\tau \quad (8)$$

Using OFDM, the channel will be only time selective:

$$\mathbf{r}(t) = \mathbf{H}(t)\, \mathbf{s}(t) + \mathbf{n}(t) \quad (9)$$

Unfortunately, it is not possible to use the instantaneous channel gains under a time selective channel since the channel is changing over time in a random manner within the transmission time. Alternatively, the channel in equation (9) can be modeled as a stationary stochastic process. Under the stationarity assumption, the statistics (i.e. the mean and covariance) of the channel matrix are constant and can be estimated at the receiver instead of the deterministic channel values. However, if the MIMO channel is not stationary, then the channel statistics may also change very fast with time and, hence, further investigation of the channel stationarity is needed to examine the feasibility of the channel statistics utilization.

In the next sections, we will try to investigate the stationarity of MIMO channels and find suitable methods to measure the stationarity. These methods can be applied one time for off-line recorded channels, since the non-stationarity of

MIMO channels is generally due to the non-stationarity of the spatial properties of the communication environment.

2.4 Stationarity of Radio Channels

In this section, we will discuss the stationarity of stochastic mobile channels. We will start with the SISO case then extend it to MIMO based on [**1**].

2.4.1 Stationary SISO Channels

SISO time-variant and frequency selective mobile channels can be seen as two dimensional stochastic process in t and τ. If the stochastic process is stationary, then the channel first and second order statistics are constant over absolute time and frequency. Thus, they can be utilized instead of the instantaneous values of the channel that varies over time and frequency. Typically, the second order statistics (i.e. the variance or the autocorrelation function) are used while the mean value of the mobile channel is assumed to be zero. The autocorrelation function of $h(t,\tau)$ is given by 4-dimensional function:

$$R_h(t,\tau;\Delta t,\Delta\tau) = E[h(t+\Delta t,\tau+\Delta\tau)h^*(t,\tau)]$$

If the channel is assumed to be wide sense stationary (WSS) in time, then R_h will depend on the time separation Δt only and does not depend on the absolute time t. The autocorrelation function of WSS channel can be written as:

$$R_h^{WSS}(\tau;\Delta t,\Delta\tau) = E[h(t+\Delta t,\tau+\Delta\tau)h^*(t,\tau)]$$

Furthermore, if the two signal components received with different time delays are uncorrelated, then R_h is zero for $\Delta\tau \neq 0$ and the channel is called uncorrelated scattering (US). The autocorrelation function of the wide sense stationary uncorrelated scattering (WSSUS) channel can be written as:

$$R_h^{WSSUS}(\tau;\Delta t,\Delta\tau) = R_h(\tau;\Delta t)\delta(\Delta\tau) = \mathrm{E}[h(t+\Delta t,\tau)h^*(t,\tau)]\delta(\Delta\tau)$$

It can be shown that WSSUS channels are stationary in frequency [**7**]:

$$R_H^{WSSUS}(\Delta t,\Delta f) = E[H(t,f)H^*(t+\Delta t,f+\Delta f)]$$

Therefore, the correlation function of WSSUS is also independent of the frequency. The variance of the channel is a constant value and can be found by setting $\Delta t = \Delta f = 0$ .The double Fourier transform of $R_H^{WSSUS}(\Delta t,\Delta f)$ with respect to Δt and Δf is called the scattering function and it is given by:

$$C_h^{WSSUS}(\tau, v) = \iint R_h(\Delta t, \Delta f)\, e^{-j2\pi v \Delta t} e^{-j2\pi \tau \Delta f}\, d\Delta t\, d\Delta f$$

where v is the Doppler frequency shift. This function shows the signal power for different time delays and Doppler shifts. In the WSSUS case, we see that the scattering function is independent of time and frequency.

2.4.2 Non- Stationary SISO Channels

Unfortunately, mobile radio channels are not WSSUS over all time and frequency periods. As the communication environment may has different propagation conditions, the channel statistics change accordingly. Instead, the channel is assumed quasi-WSSUS (QWSSUS). This implies that the channel can be assumed WSSUS within a limited time and bandwidth, so-called *stationarity region*. If the stationarity region is sufficiently large, the channel statistics can be exploited at the receiver and transmitter. On the other hand, for relatively short stationarity region, the channel statistics change very quickly and it is not possible to exploit the channel statistics at the transmitter. Thus, it is important to examine and measure the stationarity regions.

For non-WSSUS channels, a local correlation function (LCF) that depends on time and frequency is given as:

$$R_H(t, f, \Delta t, \Delta f) = E[H(t, f) H^*(t + \Delta t, f + \Delta f)]$$

The stationarity time T_s and bandwidth B_s is defined as:

$$R_H(t_1, f, \Delta t, \Delta f) \approx R_H(t_2, f, \Delta t, \Delta f) \text{ for } |t_1 - t_2| < T_s$$

$$R_H(t, f_1, \Delta t, \Delta f) \approx R_H(t, f_2, \Delta t, \Delta f) \text{ for } |f_1 - f_2| < B_s$$

Within the stationarity time and bandwidth, the autocorrelation function can be assumed constant:

$$R_H(t_1, f_1, \Delta t, \Delta f) \approx R_H(t_2, f_2, \Delta t, \Delta f) \text{ for } |t_1 - t_2| < T_s \text{ and } |f_1 - f_2| < B_s$$

For the SISO case, an estimation of the stationarity region for a non-WSSUS correlation function was introduced in [**4**][**8**]. Based on this, a channel correlation function in time, frequency, time delay and Doppler is given as:

$$A_h(\Delta t, \Delta f; \Delta \tau, \Delta v) = \iint R_h(t, f; \Delta t\, , \Delta f)\, e^{-j2\pi(t\Delta v - f\Delta \tau)}\, dt\, df$$

where A_h is called the Channel Correlation Function (CCF). The maximum time delay separation for which A_h is approximately nonzero is denoted by $\Delta\tau_{max}$ while the maximum Doppler separation for which A_h is nonzero denoted by Δv_{max}. According to [**4**], the stationarity time T_s and the stationarity bandwidth B_s are defined by:

$$T_s \triangleq \frac{1}{\Delta v_{max}}, \qquad B_s \triangleq \frac{1}{\Delta\tau_{max}}$$

If the channel is WSSUS, then $\Delta\tau_{max} = \Delta v_{max} = 0$.

2.4.3 Doubly Underspread

One important property of non-WSSUS channels is called Doubly Underspread [**9**]. If the quasi-stationarity region of the non-WSSUS is much larger than the coherence region, then the non-WSSUS channel can be called Doubly Underspread (DU). This property is very useful when channel averaging around some stationarity region is needed. If the channel is DU, then the number of independent fading realizations within the stationarity region is large. Therefore, averaging around the stationarity region is sufficient in this case since the stationarity region contains a large number of independent fading realizations. The DU channel condition is given by:

$$T_s B_s \gg T_c B_c \gg 1 \qquad (10)$$

According to [**9**] and [**1**], if the channel is not Doubly Underspread, then the estimation of the CCF from a single channel realization may not be reliable.

2.5 Stationary MIMO Channels

The investigation of MIMO channels non-stationarity has been introduced by Herdin [**1**], where the LCF and the CCF have been extended and simplified for MIMO channels.

The MIMO channel matrix in equation (6) can be formulated as 4-dimensional function in time, frequency, transmit and receive antenna domain:

$$H(t, f, n_T, n_R) = \int_{\tau=-\infty}^{\infty} h_{n_R n_T}(t, \tau)\, e^{-j2\pi f \tau}\, d\tau$$

In order to find the full correlation function of MIMO channels, we must consider the correlations among all the four dimensions of the channel. As found in [**1**], the correlation function R_H of MIMO channels is given as 8-dimensional function and can be written as:

$$R_H(t_1, t_2, f_1, f_2, n_{T,1}, n_{T,2}, n_{R,1}, n_{R,2}) = \mathrm{E}\left[H(t_2, f_2, n_{T,2}, n_{R,2}) H^*(t_1, f_1, n_{T,1}, n_{R,1})\right] \quad (11)$$

For stationary MIMO channels in all the 4-dimensions, the correlation function depends on the separation in all the four dimensions and does not depend on the absolute dimension:

$$R_H^S(\Delta t, \Delta f, \Delta n_T, \Delta n_R) = E\left[H(t_2, f_2, n_{T,2}, n_{R,2}) H^*(t_1, f_1, n_{T,1}, n_{R,1})\right]$$

However, for a non-uniform antenna array (i.e. the spacing in-between antennas is not the same), the separation in the antenna domain is different for different antennas. In this case, the correlation function is often not stationary in the antenna domain. Therefore, only time-frequency stationarity can be assumed:

$$R_H^S(\Delta t, \Delta f, n_{T,1}, n_{T,2}, n_{R,1}, n_{R,2}) = E\left[H(t_2, f_2, n_{T,2}, n_{R,2}) H^*(t_1, f_1, n_{T,1}, n_{R,1})\right] \quad (12)$$

By setting $\Delta t = \Delta f = 0$, the variance of the WSSUS MIMO channel is given as:

$$R_H^S(n_{T,1}, n_{T,2}, n_{R,1}, n_{R,2}) = E\left[H(n_{T,2}, n_{R,2}) H^*(n_{T,1}, n_{R,1})\right] \quad (13)$$

and is called the full correlation matrix. In order to simplify the estimation of equation (13) further, different MIMO channel models were proposed, as will be described in the next section.

2.6 MIMO Channel Models

In order to estimate the spatial correlation function of equation (12), we need to find a suitable analytical model to simplify it. Based on what is found in [**2**] and [**10**], two basic models will be illustrated: the full spatial correlation channel model and the Kronecker MIMO channel model. Both of the two models assume that the MIMO channel is stationary in time and frequency.

2.6.1 The Full Spatial Correlation Channel Model

In the full spatial correlation channel model, the channel correlation matrix $\mathbf{R}_H$ (also called the full correlation matrix) is given by:

$$\mathbf{R}_H = E[\mathrm{vec}\{\mathbf{H}\}\mathrm{vec}\{\mathbf{H}\}^H]$$

where $\mathbf{H}$ is $n_R \times n_T$ MIMO channel matrix with n_R receive antennas and n_T transmit antennas. Since $\mathrm{vec}\{\mathbf{H}\}$ has $n_R n_T$ elements, $\mathbf{R}_H$ will have $n_R n_T \times n_R n_T$ elements which are very large and increase rapidly as we increase the number of antennas at the transmit or receive side.

2.6.2 The Kronecker Channel Model

On the other hand, Kronecker MIMO channel model has the following channel correlation matrix:

$$\mathbf{R}_H = \frac{1}{\mathrm{tr}\{\mathbf{R}_{Rx}\}}\mathbf{R}_{Tx} \otimes \mathbf{R}_{Rx}$$

where $\otimes$ is the Kronecker product, $\mathbf{R}_{Tx}$ and $\mathbf{R}_{Rx}$ are the transmit and receive correlation matrices, respectively. They can be separate from each other as the following:

$$\mathbf{R}_{Tx} \triangleq E[\mathbf{H}^T\mathbf{H}^*] \text{ , and } \mathbf{R}_{Rx} \triangleq E[\mathbf{H}\mathbf{H}^H]$$

where $\mathbf{R}_{Tx}$ and $\mathbf{R}_{Rx}$ are $n_T \times n_T$ and $n_R \times n_R$ matrix respectively. In this way, we deal only with ${n_T}^2 + {n_R}^2$ elements divided in two matrices instead of $(n_R n_T)^2$ elements in the previous model. The major disadvantage of this simplified model is the low accuracy in describing a real MIMO channel particularly if the number of antennas is increased[**11**]. However, in this thesis we use this model for non-stationarity evaluation and not for capacity estimation.

2.7 Non-Stationary MIMO Channels

In [**1**], the local correlation function R_H of the non-stationary MIMO channel is given as 8-dimensional function:

$$R_H(t_1, t_2, f_1, f_2, n_{T,1}, n_{T,2}, n_{R,1}, n_{R,2}) = E\left[H(t_2, f_2, n_{T,2}, n_{R,2}) H^*(t_1, f_1, n_{T,1}, n_{R,1})\right] \quad (14)$$

The CCF of MIMO channel is also 8-dimensional and therefore the estimation of it is too complex. Unfortunately, estimating the CCF or LCF from a single MIMO channel realization, according to [**1**], is impassible. Therefore, we have to limit the correlation function to either time-frequency correlation over t and f, or spatial correlation over n_T and n_R. However, the spatial structure of the channel plays a central role in MIMO systems. For instance, some techniques like spatial multiplexing and beamforming (as seen in Sec. 2.2.2) are strongly sensitive to the changes of the spatial structure of the MIMO channel. Consequently, MIMO stationarity is evaluated mainly through the correlations in the spatial domain and hence equation (11) can be simplified to:

$$R_H(t, f, n_{T,1}, n_{T,2}, n_{R,1}, n_{R,2}) = E\left[H(t, f, n_{T,2}, n_{R,2}) H^*(t, f, n_{T,1}, n_{R,1})\right]$$

Alternatively, R_H can be rewritten in square matrix form of size $n_R n_T \times n_R n_T$ as:

$$\mathbf{R}_H(t, f) = E[\mathrm{vec}\{\mathbf{H}(t, f)\}\mathrm{vec}\{\mathbf{H}(t, f)\}^H] \quad (15)$$

It is possible to estimate $\mathbf{R}_H(t, f)$ in equation (15) from one time-frequency channel realization $\mathbf{H}(t, f)$. If we assume that the spatial correlation matrix $\mathbf{R}_H(t, f)$ does not change (i.e. the channel is stationary) within some averaging time T_v and bandwidth B_v (more details will be given in Sec. 3.3). In this case, we can rewrite $\mathbf{R}_H(t, f)$ as a discrete time-frequency function as:

$$\mathbf{R}_H(n, m) = E_t\left[E_f[\mathrm{vec}\{\mathbf{H}(t, f)\}\mathrm{vec}\{\mathbf{H}(t, f)\}^H]\right] \quad \text{for } t \in [nT_v, (n+1)T_v],\ f \in [mB_v, (m+1)B_v] \quad (16)$$

The spatial correlation may be different for different values of n and m. If the averaging bandwidth B_v is larger than the channel bandwidth, then equation (16) can be reduced to $\mathbf{R}_H(n)$ as:

$$\mathbf{R}_H(n) = E_t\left[E_f[\text{vec}\{\mathbf{H}(t,f)\}\text{vec}\{\mathbf{H}(t,f)\}^H]\right]$$

$$\text{for } t \in [nT_v, (n+1)T_v],\ f \in [0, B] \qquad (17)$$

where B is the channel bandwidth. Moreover, $\mathbf{R}_H(n)$ can be separated to $\mathbf{R}_{Tx}(n)$ and $\mathbf{R}_{Rx}(n)$, as discussed in Sec. 2.6.2.

2.7.1 Stationarity Region for MIMO channel

The spatial stationarity region of a MIMO channel $\mathbf{H}(t,f)$ can be defined as the region (time or distance in meters) at which the correlation matrix described by $\mathbf{R}_H(n)$ stays constant:

$$\mathbf{R}_H(n_1) = \mathbf{R}_H(n_2) \text{ for } |n_1 - n_2|T_v < T_s$$

This can be estimated by comparing two correlation matrices $\mathbf{R}_H(n_1)$ and $\mathbf{R}_H(n_2)$ that corresponds to two different regions.

Consequently, we need to define a function that compares two matrices and produces a value that is proportional to the dissimilarity between them, we call it *Matrix Metric*. This comparing function will be denoted by $M(\mathbf{R}_H(n_1), \mathbf{R}_H(n_2))$ and it ranges from a minimum value of zero (in this case we can say $\mathbf{R}_H(n_1)$ and $\mathbf{R}_H(n_2)$ are similar) to a maximum value of one for totally different matrices.

The matrix metrics can be formulated in different ways depending on the transmission technique, channel type and sensitivity to different parameters. In the following section, we will cover some of the matrix metrics and illustrate the properties and performance of each one of them.

2.8 Matrix Metrics Methods

2.8.1 Correlation Matrix Distance (CMD)

The Correlation Matrix Distance (CMD) proposed by [**1**] is one method to compare two matrices. Basically, it measures the dissimilarity between two matrices using the inner product between them. If we have two different matrices $\mathbf{R}(k)$ and $\mathbf{R}(l)$ both of them have the same size ($n \times n$), then the inner product of them is defined by:

$$\langle \mathrm{vec}(\mathbf{R}(k)), \mathrm{vec}(\mathbf{R}(l)) \rangle = \sum_i \sum_j r_{ij}(k) r_{ij}(l) = \mathrm{tr}\{\mathbf{R}(k)\mathbf{R}(l)\} \quad (18)$$

The maximum value of the inner product above can be given using Cauchy-Schwarz inequality as:

$$\mathrm{tr}\{\mathbf{R}(k)\mathbf{R}(l)\} \leq \|\mathbf{R}(k)\|_F \|\mathbf{R}(l)\|_F$$

$$\Rightarrow \quad \frac{\mathrm{tr}\{\mathbf{R}(k)\mathbf{R}(l)\}}{\|\mathbf{R}(k)\|_F \|\mathbf{R}(l)\|_F} \leq 1$$

where $\|\cdot\|_F$ is the Frobenius norm. The equality of the above holds if $\mathbf{R}(k) = \mathbf{R}(l)$. Accordingly, the CMD between two positive semi-definite Hermitian matrices $\mathbf{R}(k)$ and $\mathbf{R}(l)$ is given by:

$$CMD\big(\mathbf{R}(k), \mathbf{R}(l)\big) = 1 - \frac{\mathrm{tr}\{\mathbf{R}(k)\mathbf{R}(l)\}}{\|\mathbf{R}(k)\|_F \|\mathbf{R}(l)\|_F}$$

The CMD can ranges from zero to one. Apparently, the CMD is inversely proportional to the inner product of the two matrices. If the two matrices are orthogonal, the inner product between them will be zero and the CMD will be equal to 1. This indicates that the two matrices are totally different in the sense of dot product. On the other hand, if the two matrices are parallel, the normalized inner product of the will be equal to 1 while the CMD will be zero, indicating that the two matrices are equal.

However, CMD may not be very precise in evaluating the non-stationarity of MIMO channel. For instance, if the two correlation matrices are full rank then CMD can be very small even if the two matrices are different. Moreover, during our evaluation of the outdoor measured MIMO channel, CMD rarely exceeds 0.7 and never achieves 0.9. Therefore, we will try to find different methods to compare two matrices and then we will use it to evaluate the non-stationarity of the measured MIMO channel.

2.8.2 Normalized Correlation Matrix Distance (NCMD)

In general, if we have a matrix $\mathbf{R}(k)$, then there is a nonzero matrix $\mathbf{R}(l)$ such that the CMD value between them is 1, (i.e. $\mathbf{R}(k)$ and $\mathbf{R}(l)$ are orthogonal and the inner product $\mathrm{tr}\{\mathbf{R}(k)\mathbf{R}(l)\} = 0$). However, since the correlation matrices have a particular structure, the maximum possible CMD value for a correlation matrix $\mathbf{R}(k)$ may be less than one for any positive semi-definite Hermitian matrix $\mathbf{R}(l)$. In this case, we need to divide the CMD with a normalization factor so that the maximum difference between the correlation matrices can achieve 1.

In order to find the normalization factor, we need to find the maximum value of the CMD given one of the correlation matrices (in our case $\mathbf{R}(k)$). The second matrix $\mathbf{R}(l)$ can be any Hermitian nonzero matrix. Mathematically, we have the following maximization problem:

$$\max_{\|\mathbf{R}(l)\|_F \neq 0} CMD\big(\mathbf{R}(k), \mathbf{R}(l)\big) = \max_{\|\mathbf{R}(l)\|_F \neq 0} \left(1 - \frac{\mathrm{tr}\{\mathbf{R}(k)\mathbf{R}(l)\}}{\|\mathbf{R}(k)\|_F \|\mathbf{R}(l)\|_F}\right)$$

Alternatively, we can minimize the inner product term as:

$$\min_{\|\mathbf{R}(l)\|_F \neq 0} \frac{\mathrm{tr}\{\mathbf{R}(k)\mathbf{R}(l)\}}{\|\mathbf{R}(k)\|_F \|\mathbf{R}(l)\|_F} \qquad (19)$$

The exact solution of the above equation is rather difficult. If we take the gradient of the above equation with respect to every $r_{ij}(l)$ element and equate it with zero, we will end up with a nonlinear equation that depends on the remaining unknown $\mathbf{R}(l)$ elements. However, without the loss of generality, a solution can be found by making the following assumptions:

$$\mathbf{R}(k) \triangleq \mathbf{U}\boldsymbol{\Lambda}(k)\mathbf{U}^H$$

$$\mathbf{R}(l) \triangleq \mathbf{U}\boldsymbol{\Lambda}(l)\mathbf{U}^H$$

where $\mathbf{U}$ is an unitary matrix, $\boldsymbol{\Lambda}(k)$ and $\boldsymbol{\Lambda}(l)$ is a diagonal matrix containing the eigenvalues of $\mathbf{R}(k)$and $\mathbf{R}(l)$, respectively. The eigenvalues in $\boldsymbol{\Lambda}(k)$ and $\boldsymbol{\Lambda}(l)$ are sorted in decreasing order from maximum λ_1 to minimum λ_n. Substitute the above in the equation (18) we have:

$$\begin{aligned}\mathrm{tr}\{\mathbf{R}(k)\mathbf{R}(l)\} &= \mathrm{tr}\{\mathbf{U}\boldsymbol{\Lambda}(k)\mathbf{U}^H\,\mathbf{U}\boldsymbol{\Lambda}(l)\mathbf{U}^H\} = \mathrm{tr}\{\mathbf{U}\boldsymbol{\Lambda}(k)\boldsymbol{\Lambda}(l)\mathbf{U}^H\} \\ &= \mathrm{tr}\{\boldsymbol{\Lambda}(k)\boldsymbol{\Lambda}(l)\} = \sum_{i=1}^{n} \lambda_i(k)\,\lambda_i(l)\end{aligned} \qquad (20)$$

In order to make equation (19) as small as possible, we can set $\lambda_i(l) = 0$ for all $i \neq n$ except for $\lambda_n(l)$ which can be chosen to be any value larger than zero since it corresponds to the smallest eigenvalue of $\mathbf{R}(k)$. In this case, we can write equation (19) as:

$$\min_{\|\mathbf{R}(l)\|_F \neq 0} \frac{\mathrm{tr}\{\mathbf{R}(k)\mathbf{R}(l)\}}{\|\mathbf{R}(k)\|_F \|\mathbf{R}(l)\|_F} = \frac{\lambda_n(k)\,\lambda_n(l)}{\|\mathbf{R}(k)\|_F \|\mathbf{R}(l)\|_F} = \frac{\lambda_n(k)}{\|\mathbf{R}(k)\|_F} \qquad (21)$$

where the last equality is due to $\|\mathbf{R}(l)\|_F = \lambda_n(l)$. The solution in equation (21) holds for any Hermitian matrix $\mathbf{R}(k)$. In general, equation (20) can be rewritten as:

$$\begin{aligned} \mathrm{tr}\{\mathbf{R}(k)\mathbf{R}(l)\} &= \mathrm{tr}\{\mathbf{R}(k)\mathbf{U}\boldsymbol{\Lambda}(l)\mathbf{U}^H\} = \mathrm{tr}\{\mathbf{U}^H\mathbf{R}(k)\mathbf{U}\boldsymbol{\Lambda}(l)\} \\ &= [\mathbf{U}^H\mathbf{R}(k)\mathbf{U}]_{nn}\,\lambda_n(l) \end{aligned} \qquad (22)$$

where $[\cdot]_{ij}$ refers to the entry at row i and column j. If $\mathbf{u}_i$ is the ith column of $\mathbf{U}$, then the last term of equation (22) can be simplified as:

$$\mathrm{tr}\{\mathbf{R}(k)\mathbf{R}(l)\} = [\mathbf{U}^H\mathbf{R}(k)\mathbf{U}]_{nn}\,\lambda_n(l) = \mathbf{u}_n^H\mathbf{R}(k)\mathbf{u}_n\,\lambda_n(l) \qquad (23)$$

Since $\mathbf{R}(k)$ is Hermitian it can be decomposed to the following:

$$\mathbf{R}(k) = \mathbf{V}\boldsymbol{\Lambda}(k)\mathbf{V}^H = \sum_{i=1}^{n} \mathbf{v}_i\mathbf{v}_i^H\,\lambda_i(k) \qquad (24)$$

Substituting equation (24) in (23) gives:

$$\begin{aligned} \mathrm{tr}\{\mathbf{R}(k)\mathbf{R}(l)\} &= \sum_{i=1}^{n} \mathbf{u}_n^H\mathbf{v}_i\mathbf{v}_i^H\mathbf{u}_n\,\lambda_i(l)\,\lambda_n(k) = \sum_{i=1}^{n} (\mathbf{u}_n^H\mathbf{v}_i)^2\,\lambda_i(l)\,\lambda_n(k) \\ &\leq \lambda_n(l)\,\lambda_n(k)\sum_{i=1}^{n} (\mathbf{u}_n^H\mathbf{v}_i)^2 = \lambda_n(l)\,\lambda_n(k) \end{aligned} \qquad (25)$$

where that last equality holds since $\mathbf{v}_i$ is orthonormal for all i and hence $\sum_{i=1}^{n}(\mathbf{u}_n^H\mathbf{v}_i)^2 = 1$ for any vector $\mathbf{u}_n$ such that $\|\mathbf{u}_n\|_2 = 1$. Substituting equation (25) in (19) gives the same result of equation (21).

Consequently, the maximum value of the CMD is:

$$\max_{\|\mathbf{R}(l)\|_F \neq 0} CMD\big(\mathbf{R}(k), \mathbf{R}(l)\big) = 1 - \frac{\lambda_n(k)}{\|\mathbf{R}(k)\|_F} = 1 - \frac{\lambda_n(k)}{\sqrt{\sum_{i=1}^{n} \lambda_i^2(k)}}$$

From the above expression, we can write the new normalized CMD (NCMD) matrix metric as:

$$NCMD\big(\mathbf{R}(k),\mathbf{R}(l)\big)=\frac{CMD\big(\mathbf{R}(k),\mathbf{R}(l)\big)}{1-\dfrac{\lambda_n(k)}{\sqrt{\sum_{i=1}^{n}\lambda_i^2(k)}}}=\frac{CMD\big(\mathbf{R}(k),\mathbf{R}(l)\big)}{K_N}$$

where K_N is the normalization factor. If the smallest eigenvalue of $\mathbf{R}(k)$ is equal to zero, then the normalization factor will be equal to one and hence the NCMD is the same as CMD. On the other hand, if $\mathbf{R}(k)$ has equal eigenvalues, then the minimum value of K_N is achieved and is equal to $1-1/\sqrt{n}$.

For small values of n (i.e. small number of transmit or receive antennas), the maximum value of the NCMD is 3.4 times higher than CMD for two antenna system and 2.3 times higher for three antenna system. For our case, we have a 4x4 MIMO channel; therefore, the minimum normalization factor is 0.5 which increases the NCMD two times above CMD. However, for low rank matrices, the minimum eigenvalue is zero and, hence, both the two methods will have similar performance.

2.8.3 Distance between Equidimensional Subspaces (DES)

The last distance measure between two matrices used in this thesis is the Distance between Equidimensional Subspaces (DES) method [**12**]. In this method, we extract the eigenvectors of the two correlation matrices and take only the first p eigenvectors that correspond to the largest eigenvalues then we compare these eigenvectors based on the DES between them.

To illustrate this, let $\mathbf{R}(p)$ and $\mathbf{R}(q)$ be two Hermitian matrices to be compared. Accordingly, the $\mathbf{R}(p)$ can be written as:

$$\mathbf{R}(p)=\lambda_1(p)\mathbf{u}_1(p)\mathbf{u}_1^H(p)+\lambda_2(p)\mathbf{u}_2(p)\mathbf{u}_2^H(p)+\cdots+\lambda_n(p)\mathbf{u}_n(p)\mathbf{u}_n^H(p)$$

where $\lambda_i(p)$ and $\mathbf{u}_i(p)$ are the eigenvalue and eigenvector of $\mathbf{R}(p)$, respectively. We define $\mathbf{R}_k(p)$ as:

$$\mathbf{R}_k(p)=\lambda_1(p)\mathbf{u}_1(k)\mathbf{u}_1^H(p)+\lambda_2(p)\mathbf{u}_2(p)\mathbf{u}_2^H(p)+\cdots+\lambda_k(p)\mathbf{u}_k(p)\mathbf{u}_k^H(p)$$

where $p < n$ corresponds to the largest p eigenvalues of $\mathbf{R}(p)$. After that, we can compare $\mathbf{R}_k(p)$ and $\mathbf{R}_k(q)$ using the DES method. The distance between $\mathbf{R}_k(p)$ and $\mathbf{R}_k(q)$ can be computed by the following algorithm.

2.8.3.1 DES algorithm

1 . Compute the QR factorization of $\mathbf{R}_k(p)$ and $\mathbf{R}_k(q)$:

$$\mathbf{R}_k(p) = \mathbf{Q}(p)\mathbf{T}(p)$$

$$\mathbf{R}_k(q) = \mathbf{Q}(q)\mathbf{T}(q)$$

where $\mathbf{T}$ is upper triangular matrix. Note that the value of $\mathbf{Q}$ is $n \times k$ matrix and can be found directly as $\mathbf{Q} = [\mathbf{u}_1 \quad \mathbf{u}_2 \quad \cdots \quad \mathbf{u}_k]$.

2. Define $\mathbf{C} \triangleq \mathbf{Q}^H(p)\mathbf{Q}(q)$.

3. Find the SVD of $\mathbf{C}$: $\mathrm{SVD}(\mathbf{C}) = \mathbf{U}\boldsymbol{\Sigma}\mathbf{V}^H$

where $\boldsymbol{\Sigma}$ is a diagonal matrix. The minimum value of $\boldsymbol{\Sigma}$ is the cosine of the largest principle angle between $\mathbf{R}_k(p)$ and $\mathbf{R}_k(q)$ i.e. $\cos(\theta_{max}) = \min(\boldsymbol{\Sigma})$.

4. Calculate the DES between $\mathbf{R}_k(p)$ and $\mathbf{R}_k(q)$ as:

$$\mathrm{DES}(\mathbf{R}(p), \mathbf{R}(q), k) = \sin(\theta_{max}) = \sqrt{1 - \cos^2(\theta_{max})} = \sqrt{1 - \min(\boldsymbol{\Sigma})}$$

Chapter 3
Results

In this chapter, the matrix metric methods will be applied to realistic measured MIMO channels. Then, these methods will be compared with each other, and a short conclusion will be stated.

3.1 Measured MIMO Channel

In signal processing laboratory at KTH, we have access to a large data set of realistic measured 4x4 MIMO channels for an outdoor environment made by Ericsson Company, and applicable to LTE standard. The measurements were performed in Kista, a suburb of Stockholm city in Sweden, for a driving car scenario.

The center frequency and the bandwidth of the measured channels were 2.6 GHz and 20 MHz, respectively. Table 1 summarizes the properties of the measured used in this thesis. Note that, the measured channel matrix function is sampled in time and frequency; therefore, it can be written as a discrete function $\mathbf{H}(nT_p, mF_p)$ or simply as $\mathbf{H}(n, m)$.

The used track in this thesis is track number 3A shown in Figure 2. Additionally, we separated the track to LOS route (highlighted in dashed red) and the NLOS route (highlighted in blue) based on visual inspections.

Location	Kista, Stockholm, Sweden
Scenario	Suburban, Driving car
Transmit antennas	4 antennas , at base station
Receive antennas	4 antennas, at moving car
Center frequency f_c	2.6 GHz
Wavelength λ_c	0.115 m
Bandwidth B	20 MHz
Frequency sample spacing F_p	123 KHz
Number of frequency samples N_f	162
Time sample spacing T_p	5.33 ms
Maximum receiver speed s_{max}	35 Km/hr
Average receiver speed s_{avg}	22 Km/hr

Table 1: Properties of the measured MIMO channels

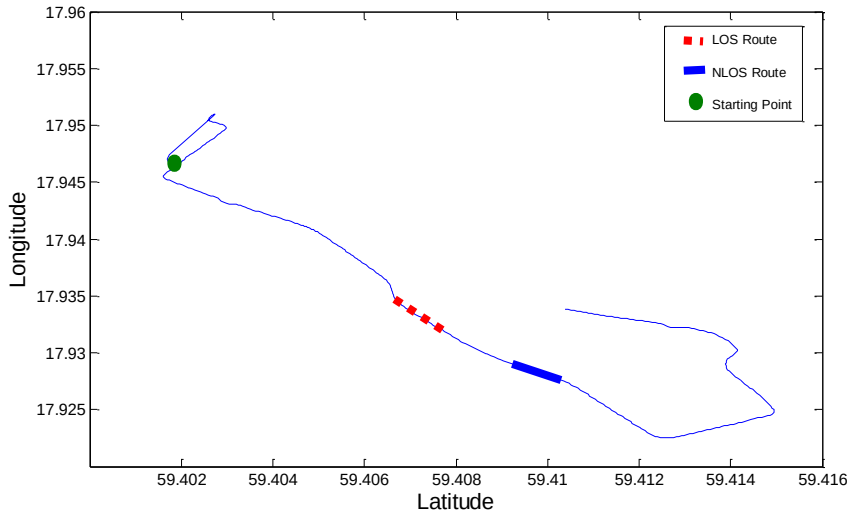

Figure 2: Track number 3A, the LOS and NLOS routes are highlighted in red and blue, respectively.

The antenna structure of the transmit antennas (at base station) and receive antennas (at the car roof) are shown in Figure 3. As shown in Figure 3, the transmit antennas are segregated to two dual polarized antennas. In this thesis, small and large spacing between the dual polarized antennas were used. However, all the non-stationarity evaluation was made with the small spacing setup while the large spacing setup was used only for comparisons in Sections 3.4.2.3 and 3.4.3.3.

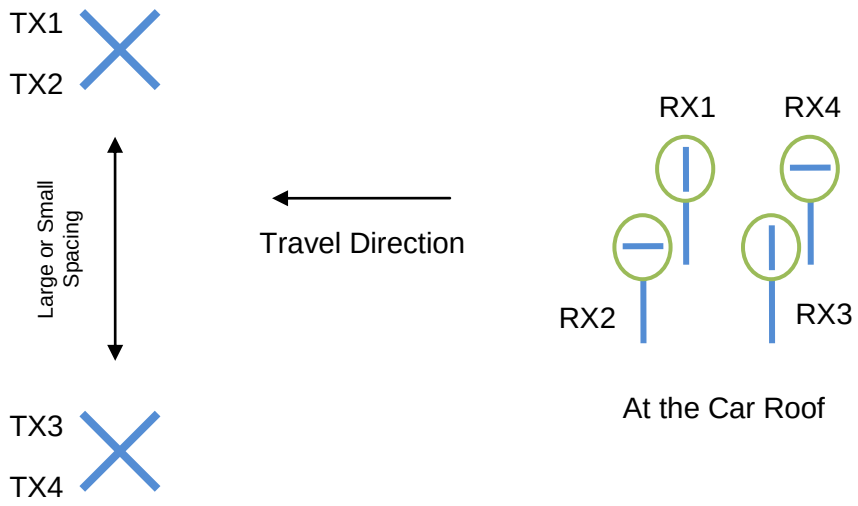

Figure 3: Antenna configuration of transmit and receive antennas.

3.2 Minimum Stationarity Region

In order to estimate the correlation matrix, we first need to find the averaging time T_v and bandwidth B_v. The averaging time and bandwidth should be sufficiently large to create a reliable estimation of the correlation matrix. However, the averaging time and bandwidth should be smaller or equal to the minimum stationarity time T_s^{min} and bandwidth B_s^{min}, respectively to ensure that the statistics of the spatial structure are constant within the averaging time and bandwidth. Therefore, we have to define roughly the minimum stationarity region of the spatial structure before we estimate the exact stationarity region.

3.2.1 Minimum Stationarity Time

The statistics of the spatial structure can be assumed constant, if the receiver move a distance less than $10\,\lambda_c$. For a moving car scenario, as the case for our channel, the stationarity time can be roughly assumed as the time that corresponds to moving $10\,\lambda_c$. Therefore, the stationarity time can be calculated as:

$$T_s^{min} \approx \frac{10\,\lambda_c}{s_{avg}} = \frac{D_s^{min}}{s_{avg}}$$

where s_{avg} is the average car speed and D_s^{min} is the minimum stationarity distance. By using the average speed of the car, the average stationarity time is about 188.8ms. However, since the speed of the car $s(t)$ is time varying, the instantaneous stationarity time is also varying. Thus, in order to make the correlation matrix independent of time, we need to express the channel as a function of distance rather than time.

Fortunately our measured channel is equipped with a GPS data showing the position of channel samples every one second. Therefore, we can average over every $D_v = D_s^{min} = 10\,\lambda_c$ meter and the correlation matrix can be expressed in term of discrete distance steps as $\mathbf{R}(d) = \mathbf{R}(D_v n)$.

3.2.2 Minimum Stationarity Bandwidth

Since the channel bandwidth is much smaller than the center frequency (the channel bandwidth is only 0.8% of the center frequency), we will assume that the spatial structure is stationary within all the channel bandwidth i.e. $B_v = B_s^{min}$ =20MHz.

3.2.3 Doubly Underspread

Recall the doubly underspread (DU) condition in equation (10) and :

$$T_v B_v \gg T_c B_c \gg 1$$

In a similar analysis to what we found in [**4**], [**13**] and [**14**], the averaging time and frequency were calculated to be 188.8ms and 20MHz, respectively. The maximum Doppler shift is can be calculated as $v_{max} = (s_{max}/c) f_c \approx 53$ Hz hence the coherence time $T_c \approx$19ms. If we assume that the maximum delay travel 2km, as the total length of the track is 1km, then the value of the coherence bandwidth $B_c = c/d$ is roughly 150kHz. Therefore, the doubly underspread is satisfied as 188ms×20MHz ≫ 19ms×150kHz = 2850 ≫ 1. The total number of independent fading realization within the stationarity time and bandwidth is about $T_v B_v / T_c B_c \approx$ 1320 realizations.

3.3 Estimation of Correlation Matrix

Before we can start non-stationarity investigation of the measured channel, we need to estimate the correlation matrix of equation (17). Nevertheless, we have one discrete time and frequency realization of the measured channel. Therefore, the spatial correlation matrix can be estimated by averaging within a stationarity region (time and frequency) in which the spatial structure of the channel can be assumed constant as:

$$\widehat{\mathbf{R}}_H(d) = \frac{1}{N_t(d)} \frac{1}{N_f} \sum_{n=1}^{N_t(d)} \sum_{m=1}^{N_f} \mathrm{vec}\{\mathbf{H}(n,m)\} \mathrm{vec}\{\mathbf{H}(n,m)\}^H$$

where $N_t(d)$ is the number of time samples within the distance $[dD_v, (d+1)D_v]$ and N_f is the number of stationary frequency samples. Alternatively, we can estimate the Kronecker transmit and receive correlation matrix as:

$$\widehat{\mathbf{R}}_{Tx}(d) = \frac{1}{N_t(d)} \frac{1}{N_f} \sum_{n=1}^{N_t(d)} \sum_{m=1}^{N_f} \mathbf{H}^{\mathrm{T}}(n,m) \mathbf{H}^{*}(n,m)$$

$$\widehat{\mathbf{R}}_{Rx}(d) = \frac{1}{N_t(d)} \frac{1}{N_f} \sum_{n=1}^{N_t(d)} \sum_{m=1}^{N_f} \mathbf{H}(n,m) \mathbf{H}^{H}(n,m)$$

3.4 Evaluation of MIMO Non-Stationarity

3.4.1 Spatial Stationary Channel

In this section, we will illustrate the performance of the matrix metrics for still transmitter and receiver to ensure proper functionality of the matrix metric functions. In the beginning of the measurements, the car was standing for 3 seconds before it starts moving. The channel has more than one multipath component and varies with frequency as shown in Figure 4.

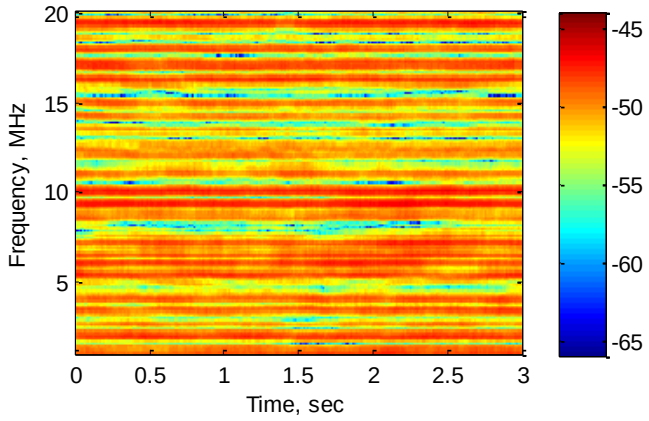

Figure 4: Spatial Stationary Channel versus time and frequency.

In order to evaluate the matrix metrics under this type of channel, the correlation matrices as a function of time ($\widehat{\mathbf{R}}_{Tx}(t)$ and $\widehat{\mathbf{R}}_{Rx}(t)$) is needed here. Figure 5 shows the matrix metrics values of the transmit and receive correlation matrices with respect to the first instant $\widehat{\mathbf{R}}(t=0)$. Here, the DES method is used with a base number k=1. Apparently from Figure 5, all the matrix metrics stay below 0.08 as an indication of spatial stationarity.

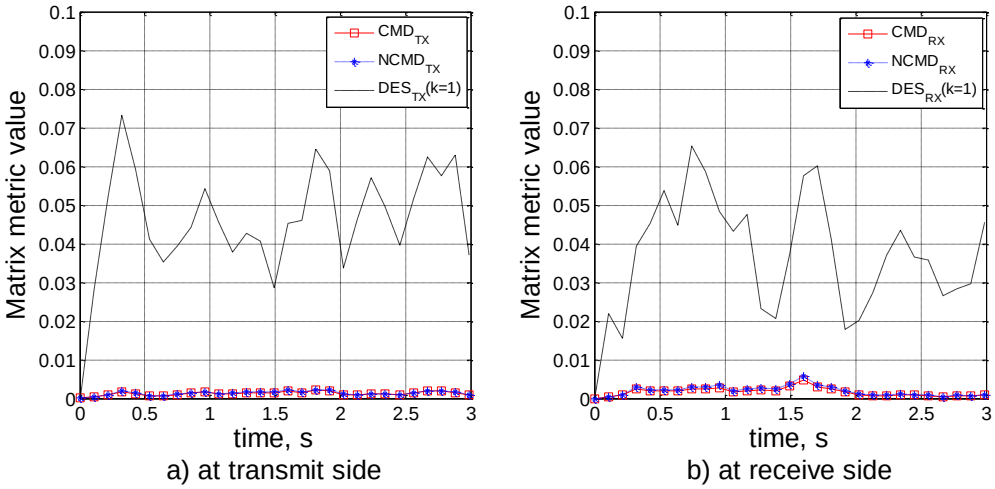

Figure 5: CMD, NCMD and DES of spatial stationary channel with respect to $\widehat{\mathbf{R}}(t=0)$.

3.4.2 LOS Channel Non-Stationarity

The LOS region of the channel was detected by visual inspection of the channel spectrogram. The frequency spectrum of the LOS channel is flat, since the LOS component with zero delay is the dominate signal while the multipath signals are much lower. Figure 6 shows the distance-frequency LOS channel spectrogram while Figure 7 shows the eigenvalues variation of $\widehat{\mathbf{R}}_{Tx}$ and $\widehat{\mathbf{R}}_{Rx}$ versus distance. In the next sections, we will evaluate the LOS non-stationarity using matrix metric methods.

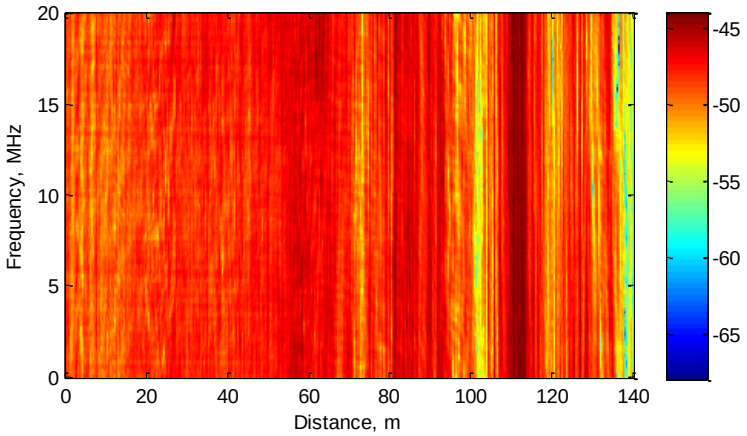

Figure 6: LOS Spectrum versus frequency and distance. The color bar shows the channel strength in dB.

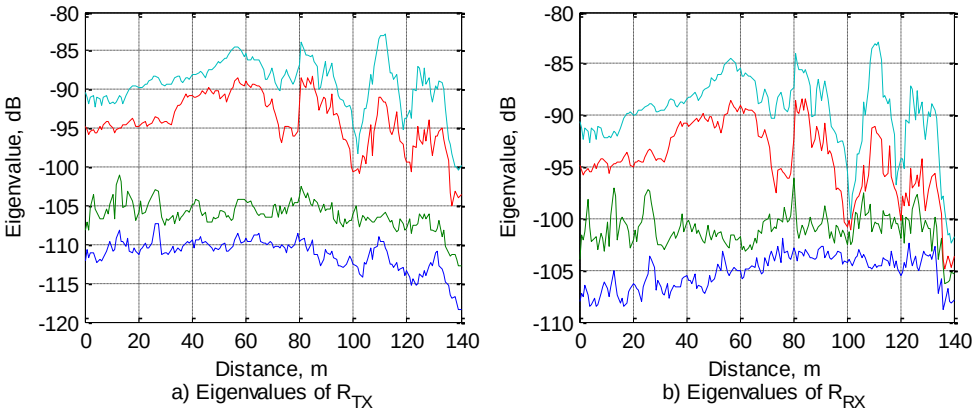

Figure 7: The eigenvalues of $\widehat{\mathbf{R}}_{Tx}$ and $\widehat{\mathbf{R}}_{Rx}$ versus distance for the LOS route.

3.4.2.1 Spatial Variation of LOS Channel

Initially, the matrix metrics for the starting point of LOS route were evaluated using the estimated correlation matrices $\widehat{\mathbf{R}}_{Tx}(d)$ and $\widehat{\mathbf{R}}_{Rx}(d)$ as a function of distance. Figure 8 shows the variation of the matrix metrics with distance when comparing the first correlation matrix $\widehat{\mathbf{R}}(0)$ with the entire route. In general, the matrix metrics increase with distance as the spatial structure variance of the channel changes. However, both the CMD and the NCMD values do not exceed 0.8 even with a large distance separation. As clearly observed from Figure 8, the NCMD method performance is very close to CMD method. In fact, the normalization factor was very close to one (0.99 and 0.98 for $\widehat{\mathbf{R}}_{Tx}(0)$ and $\widehat{\mathbf{R}}_{Rx}(0)$, respectively) due to the large ratio between the maximum and minimum eigenvalues of the correlation matrix, as seen in Figure 7. In this case, the NCMD is only 2% above CMD. On the other hand, the DES method appears to be more sensitive to the spatial variations with an average sensitivity gain of 0.2 above both the CMD and NCMD methods.

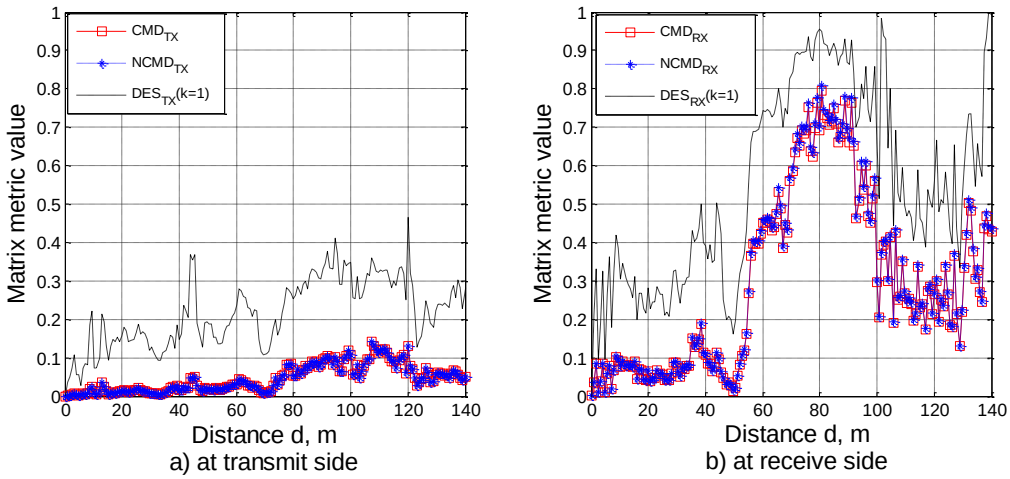

Figure 8: Different matrix metrics of the LOS route, in (a) $M(\widehat{\mathbf{R}}_{Tx}(0), \widehat{\mathbf{R}}_{Tx}(d))$ and in (b) $M(\widehat{\mathbf{R}}_{Rx}(0), \widehat{\mathbf{R}}_{Rx}(d))$.

More illustration of the matrix metrics between all distance points is given in Figure 9. In this figure, the image diagonal corresponds to the matrix metrics between two similar points where $d_1 = d_2$ and hence the matrix metrics value is zero. All the images show distinct sections of the spatial structure. For NCMD method at transmit side, Figure 9.a shows that the whole LOS route is stationary. On the other hand, the receive side in Figure 9.b has 6 separate stationarity sections that have similar spatial properties (the largest one is approximately from 0 m to 50 m).

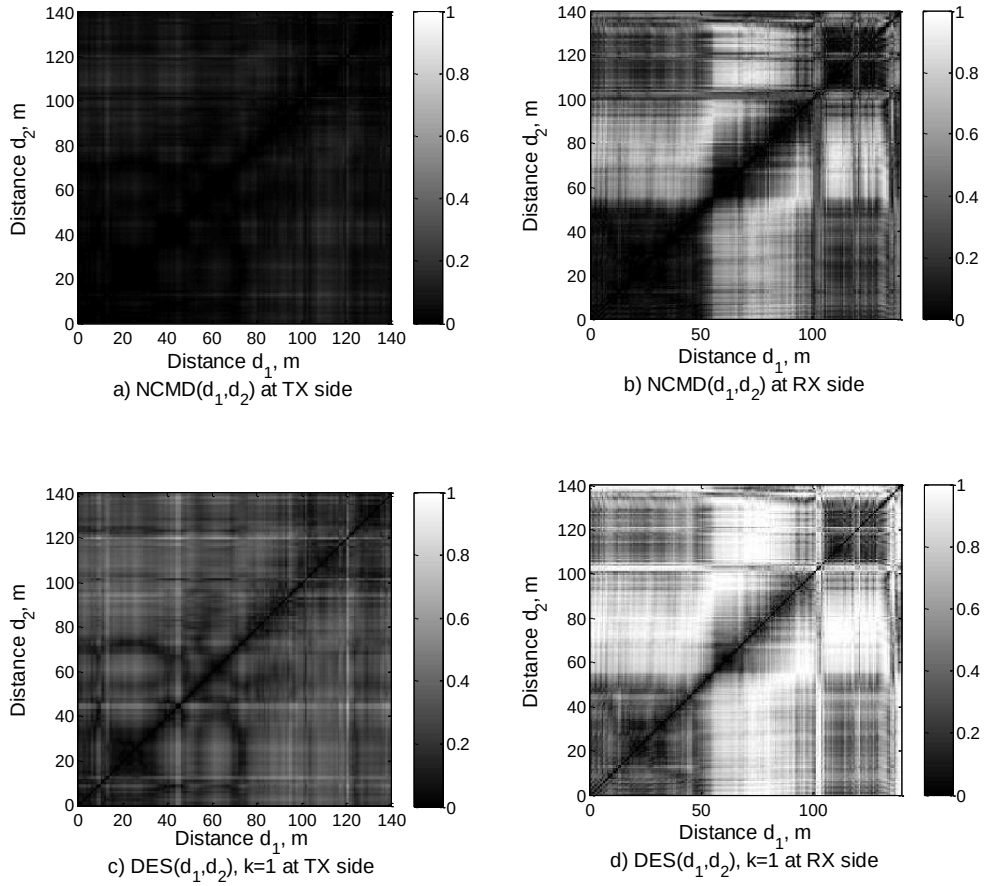

Figure 9: The NCMD and DES values between all distance points of the LOS route.

On the other hand, the DES method shows more details for different spatial sections. Comparing the NCMD with DES of the receiver side (Figure 9.b and Figure 9.d), it can be seen that section [0m, 50m] seems to have one spatial structure when using NCMD method (Figure 9.b) while the same section appears to has different spatial structures when using DES (Figure 9.d).

3.4.2.2 LOS Channel Stationarity Distance

The local stationarity distance can be defined as the distance at which the matrix metric is lower than a certain threshold value. Mathematically, it can be expressed as:

$$D\big(\mathbf{R}(d_1)\big) = \max d_2 \text{ subject to: } M\big(\mathbf{R}(d_1), \mathbf{R}(d_2)\big) < c$$

where c is the threshold value. Recall Figure 8, if a threshold value of 0.2 is used, the stationarity distance of point zero for the DES metric is about 10 m at the transmit side. Note that, $M\big(\mathbf{R}(d_1), \mathbf{R}(d_2)\big)$ should stays below c all the way between d_1 and d_2.

Based on the pervious definition, the stationarity distance of the LOS route is calculated with a threshold value of 0.2. Figure 10 shows the local stationarity distance of different matrix metrics.

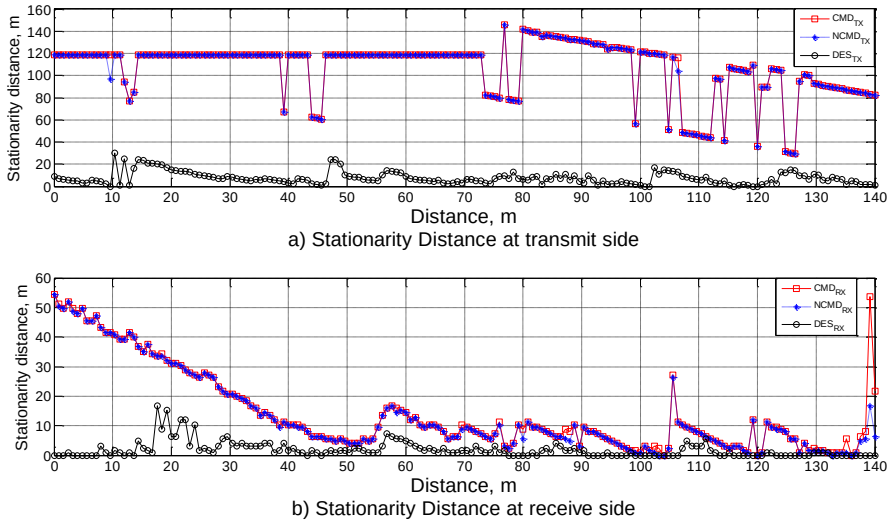

Figure 10: Local stationarity distance of different matrix metric methods in the LOS route with threshold value = 0.1.

Again, the performance of the CMD and NCMD is very similar. According to CMD and NCMD metric, it can be seen that there is more than one stationarity section in the LOS route. For illustration, section [0m, 50m] is considered to be stationary with respect to NCMD and CMD for both transmit and receive sides since the CMD value for any two points inside this section is less than 0.2. On the other hand, the DES method appears to have much lower stationarity distances with few and short stationarity sections. For some transmission scenarios,

beamforming for instance, the CMD and NCMD will give much larger estimation of the stationarity distance.

The average value and standard deviation of the CMD, NCMD and DES versus distance separation Δd of the LOS route are shown in Figure 11. The standard deviation is shown as an error bar on each point. The total number of realizations used is about 110 realizations taken from the first 110 m of the LOS route. From Figure 11, it is possible to find the stationarity distance length based on different threshold values.

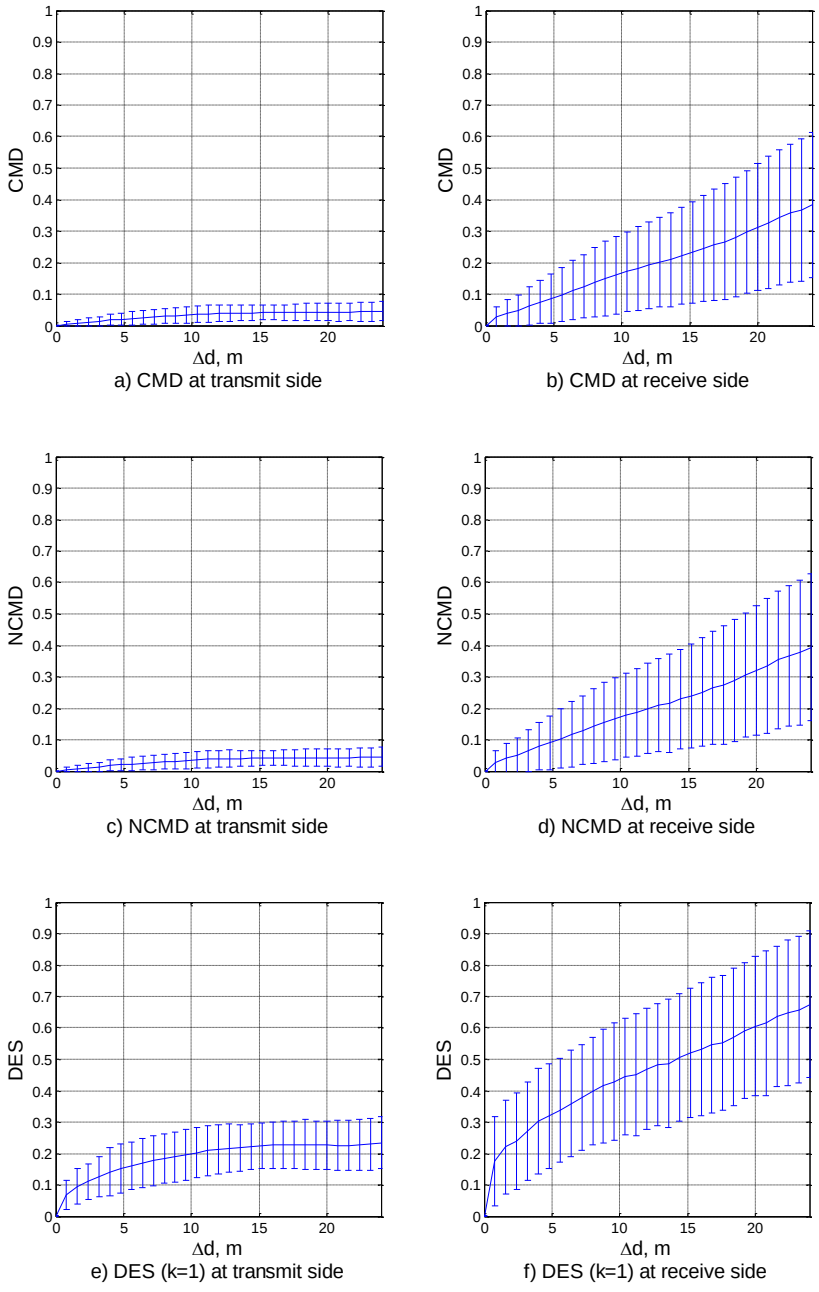

Figure 11: Mean value and standard deviation of CMD, NCMD and DES versus Δd for the LOS route.

3.4.2.3 LOS Non-Stationarity Using Different Transmit Antenna Spacing

The second measurement of the LOS route was performed with exactly the same receive antenna type while the spacing between the dual polarized antennas was increased at the transmit side. Figure 12 shows the average NCMD and DES versus the separation in distance for the small and large antenna spacing. From the figure, the large antenna spacing has increased the non-stationarity at the transmit side compared to the small antenna spacing while the non-stationarity at the receive side is exactly the same. In the small antenna spacing, all the four transmit antenna elements approximately have the same LOS path and, hence, the small antenna spacing is more stationary than the large antenna spacing.

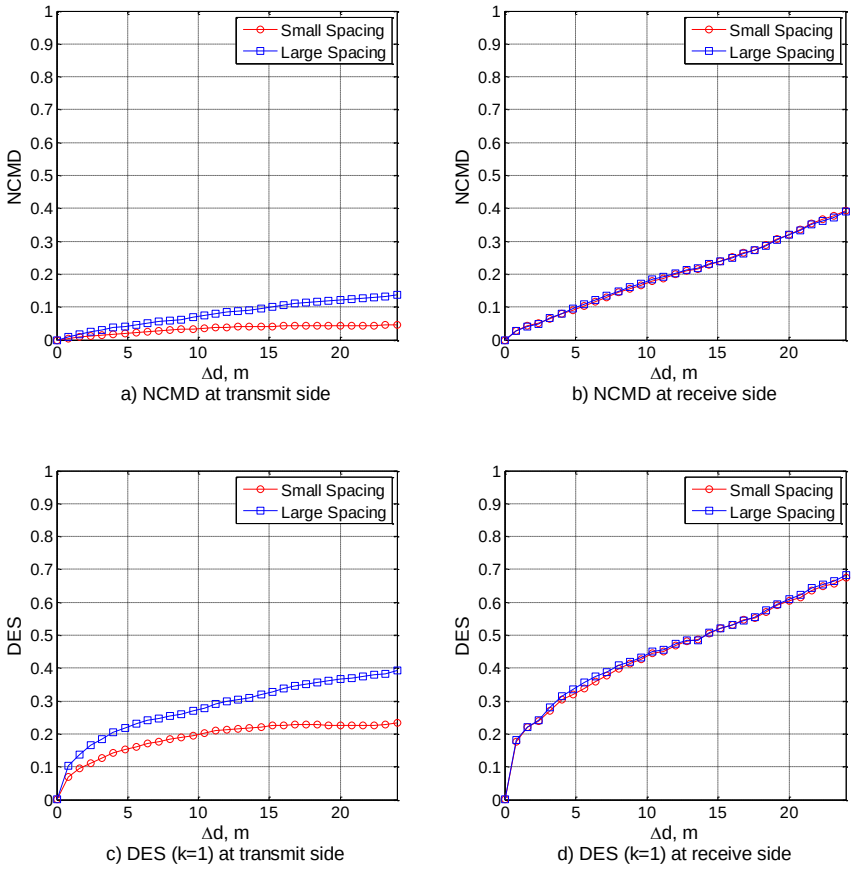

Figure 12: Distance shift versus matrix metric at transmit and receive sides of the small and large antenna spacing at the transmit side for LOS channel.

3.4.3 NLOS Channel Non-Stationarity

The NLOS channel changes rapidly with frequency and distance. In track 3A, the NLOS route was detected as shown in Figure 13. The channel data is measured using exactly the same antennas of the LOS route (small antenna spacing). Apparently, the NLOS channel has much lower signal strength than the LOS and hence much lower eigenvalues.

Figure 14 shows the average eigenvalues of $\widehat{\mathbf{R}}_{Tx}$ and $\widehat{\mathbf{R}}_{Rx}$ for NLOS channel sorted from maximum to minimum. Comparing Figure 14 with Figure 7, the NLOS channel shows more closely eigenvalues than the LOS channel. This seems to be reasonable since LOS MIMO channels are low rank, in general.

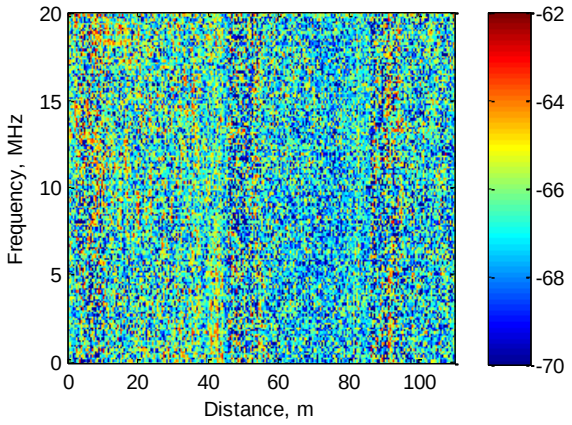

Figure 13: NLOS Spectrum versus frequency and distance. The color bar shows the channel strength in dB.

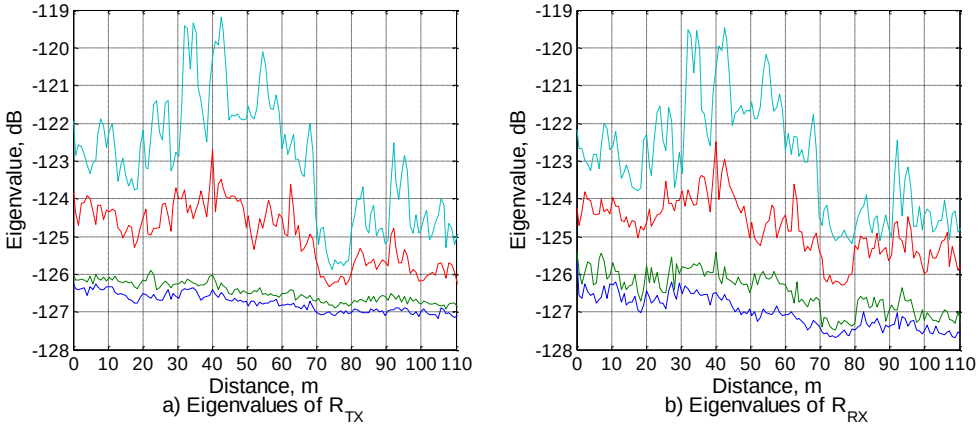

Figure 14: The eigenvalues of $\widehat{\mathbf{R}}_{Tx}$ and $\widehat{\mathbf{R}}_{Rx}$ versus distance for the NLOS route.

To evaluate the non-stationarity of the NLOS channel, the same methods used previously in LOS channel was applied here. Nevertheless, the DES method can be applied with different base number k, in this case. Since the eigenvalues of $\widehat{\mathbf{R}}_{Tx}$ are close to each other, different base number will result in different stationarity measure, as will be shown in next sections.

3.4.3.1 Evaluation of the Spatial Variation of NLOS Channel

Figure 15 shows the variation of the matrix metrics with distance of the NLOS channel when the first correlation matrix $\widehat{\mathbf{R}}(0)$ is compared with the entire route. Here, the difference between the CMD and NCMD is relatively large compared to the LOS case (the normalization factor is 0.66, and the NCMD is 50% larger than CMD at the receive side).

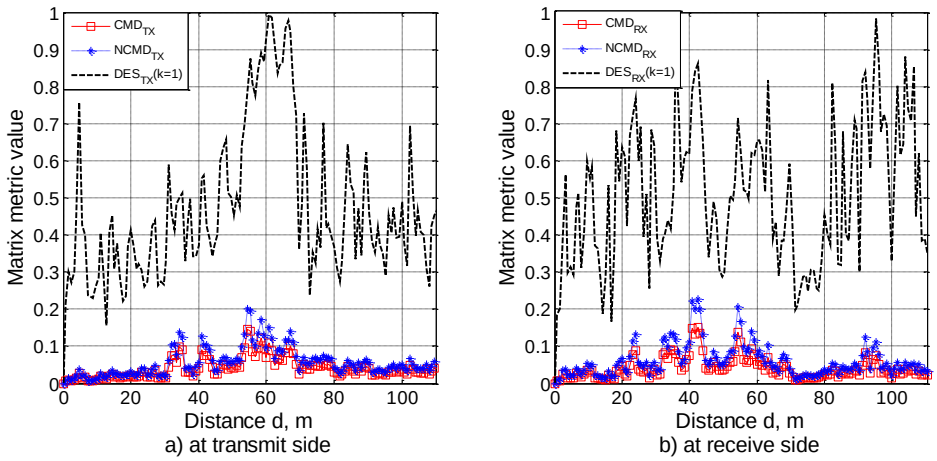

Figure 15: CMD, NCMD and DES of the NLOS with respect to $\widehat{\mathbf{R}}(0)$.

From

Figure 15.a, it is clearly that there is a large difference between DES method compared to both CMD and NCMD. The DES method with base $p = 1$ shows very large variations in the spatial structure while, in contrast, CMD and NCMD show lower spatial variation.

The performance of the DES method with different base numbers at the transmit side is shown in Figure 16. In this figure, it can be seen that different base number produces different metric methods. Since the smallest DES variation corresponds to $p = 2$, it seems that the bases of the largest two eigenvalues are interchanging with each other while the bases of the remaining eigenvalues stay below them.

Depending on the MIMO transmission scenario, different bases number can be chosen when using the DES method.

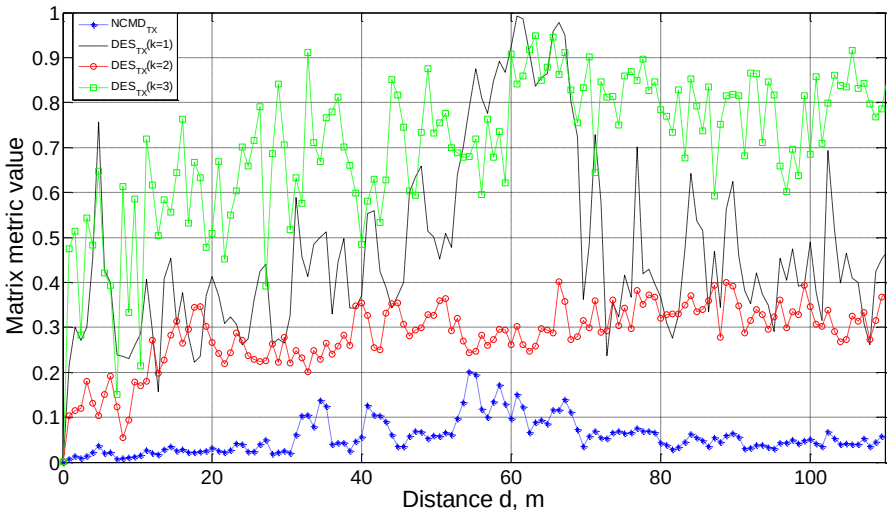

Figure 16: Different base numbers of DES of the NLOS route with respect to $\widehat{\mathbf{R}}_{Tx}(0)$.

The spatial variation at the transmit side of all points in the NLOS route with different base numbers for the DES method is shown in Figure 17. Comparing Figure 17 with Figure 9, the CMD, NCMD and DES values for the NLOS case seem to be higher than the LOS channel.

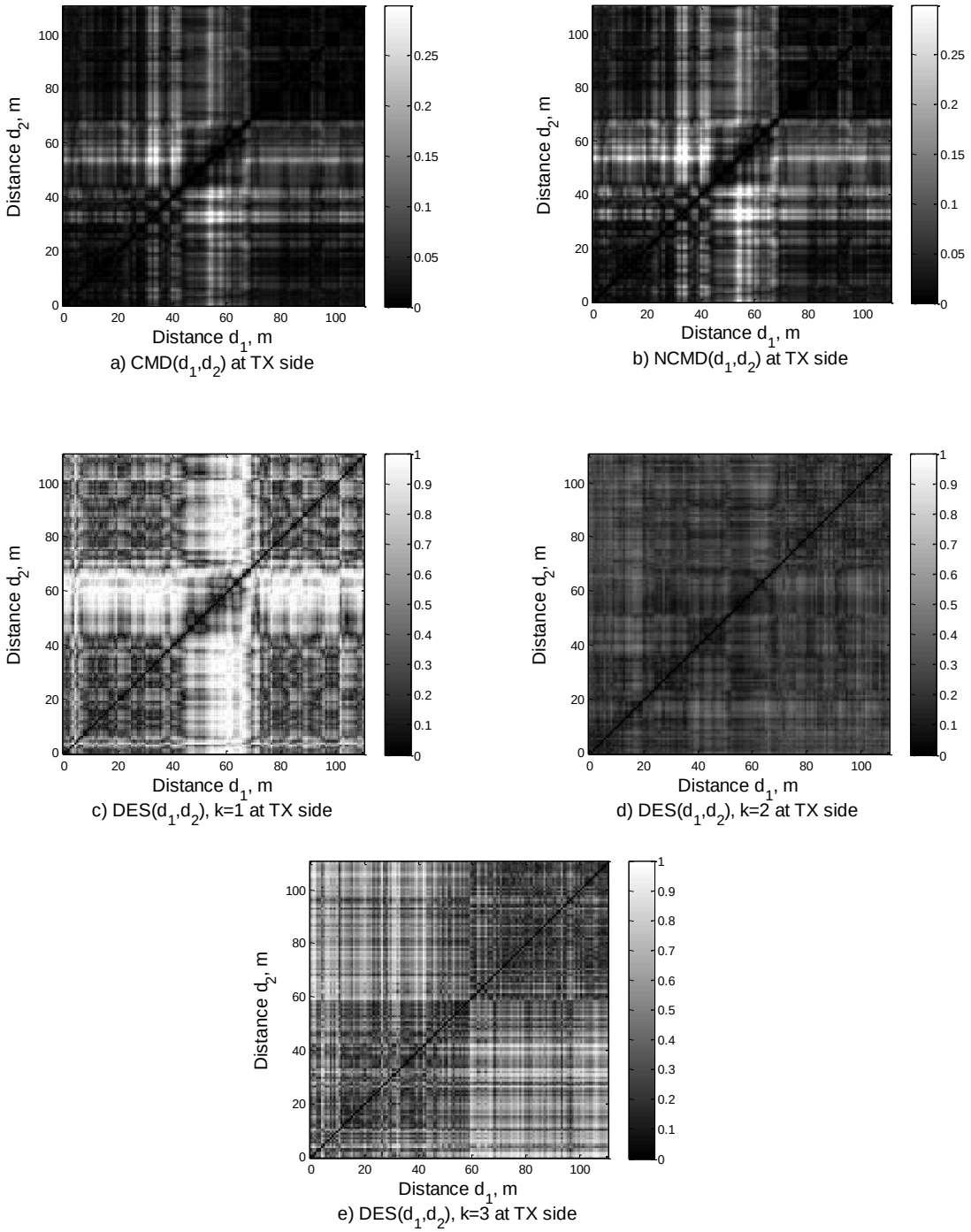

Figure 17: CMD, NCMD and DES with k = 1 to 3 between all points in the NLOS route.

3.4.3.2 Evaluation of NLOS Channel Stationarity Distance

The stationarity distance of the NLOS channel for 0.2 threshold value is shown in Figure 18. From this figure, the DES method at k = 1 shows almost no local stationarity distance for the NLOS route at both transmit and receive sides. On the other hand, CMD method shows very large stationarity distance at both sides. At the transmit side, it shows that almost the entire NLOS route is stationary with distance. Since the NLOS channel is higher in rank than the LOS channel, the CMD metric underestimate the non-stationarity by a large amount.

The stationarity distance for different base numbers for the DES method is shown in Figure 19. As expected, the less sensitive base number (k = 2) has the largest stationarity distance compared to other bases but still very low compared to CMD and NCMD.

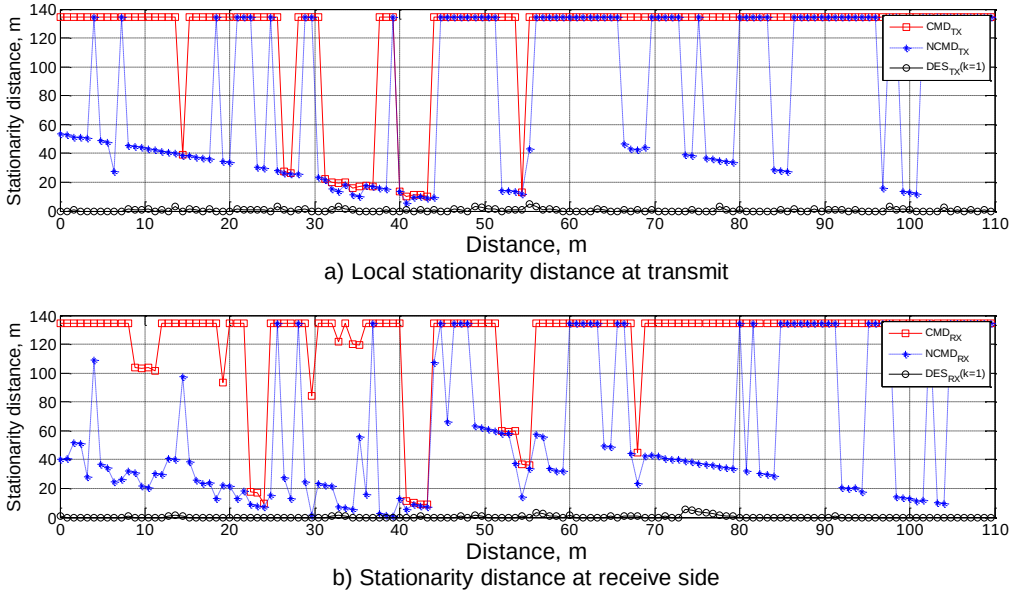

Figure 18: Local stationarity distance of CMD, NCMD and DES in the NLOS route.

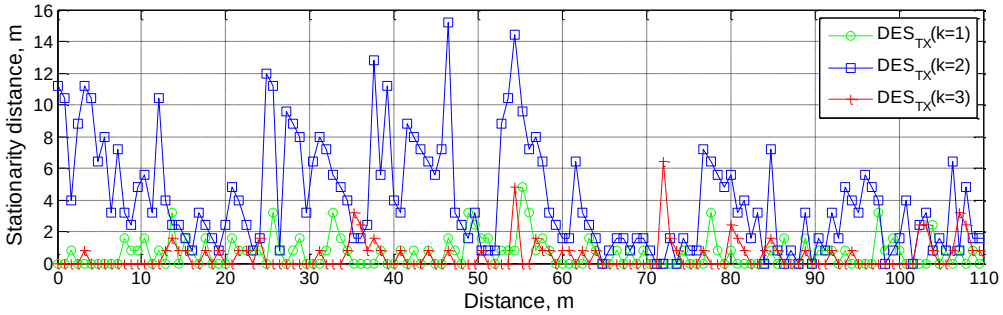

Figure 19: Local stationarity distance of different base values of DES method in the NLOS route at the receiver side.

Table 2 and Table 3 shows the average stationarity distance of the NLOS route at the transmit side and for 0.2 and 0.1 threshold value, respectively. Here, the CMD overestimates the real stationarity distance compared to the NCMD.

Matrix Metric	Average Stationarity Distance at TX (c=0.2)
CMD	120 m
NCMD	82 m
DES (k=1)	0.63 m
DES (k=2)	4 m
DES (k=3)	0.5 m

Table 2: The average stationarity distance at the transmit side of the NLOS route for 0.2 threshold value.

Matrix Metric	Average Stationarity Distance at TX (c=0.1)
CMD	40 m
NCMD	18 m

Table 3: The average stationarity distance at the transmit side of the NLOS route for 0.1 threshold value.

The mean value and standard deviation of the CMD, NCMD and DES versus the distance separation Δd at the transmit side of the NLOS route is shown in Figure 20.

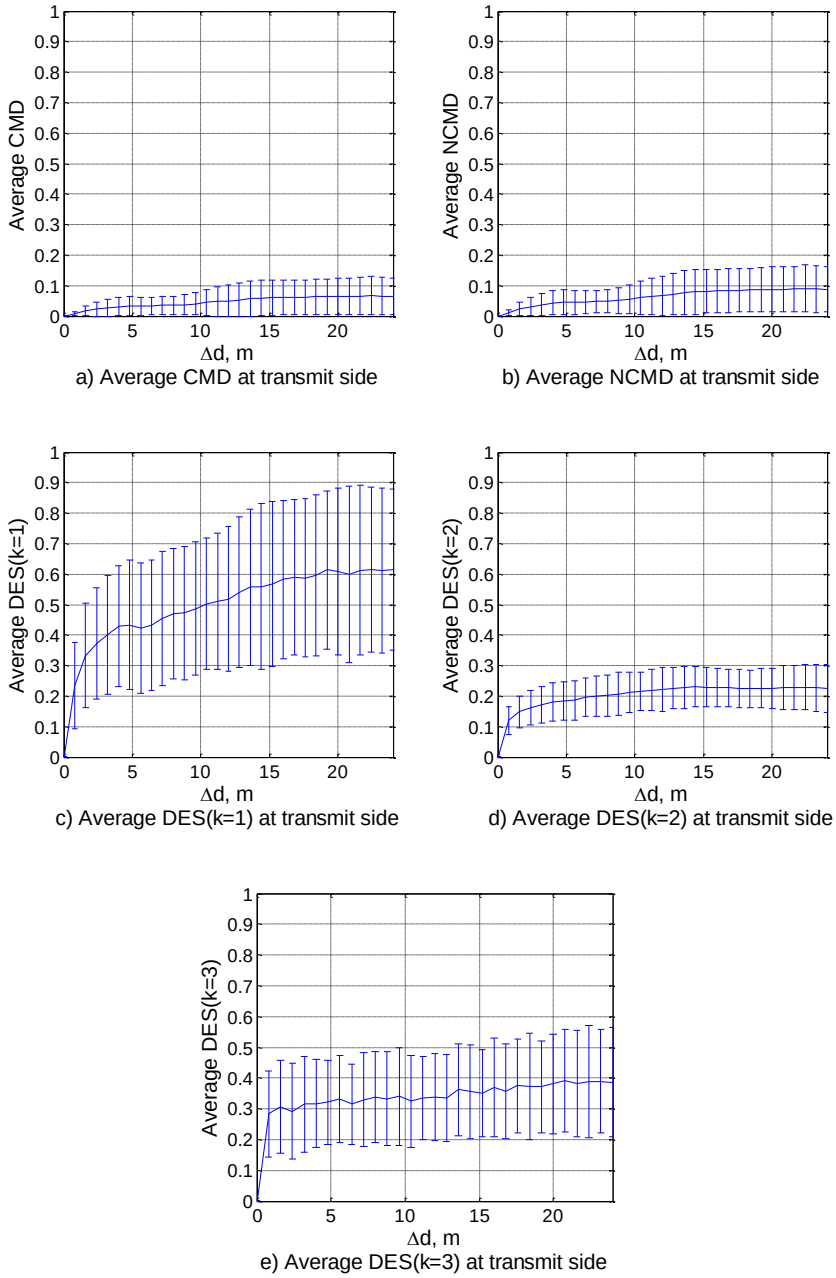

Figure 20: Mean value and standard deviation of the metric methods versus distance difference Δd for the NLOS route at the transmit side.

3.4.3.3 NLOS Non-Stationarity Using Different Transmit Antenna Spacing

The second measurement of the NLOS route was performed with exactly the same receive antenna type while the spacing between the dual polarized antennas was increased at the transmit side. Figure 21 shows the average NCMD and DES versus the separation in distance for the small and large antenna spacing. From the figure, the large antenna spacing has slightly increased the non-stationarity at the transmit side. Under the NLOS environment, the four transmit antenna elements no longer have the same path components; thus, the large spacing antenna slightly reduced the non-stationarity at the transmit side compared to the LOS case.

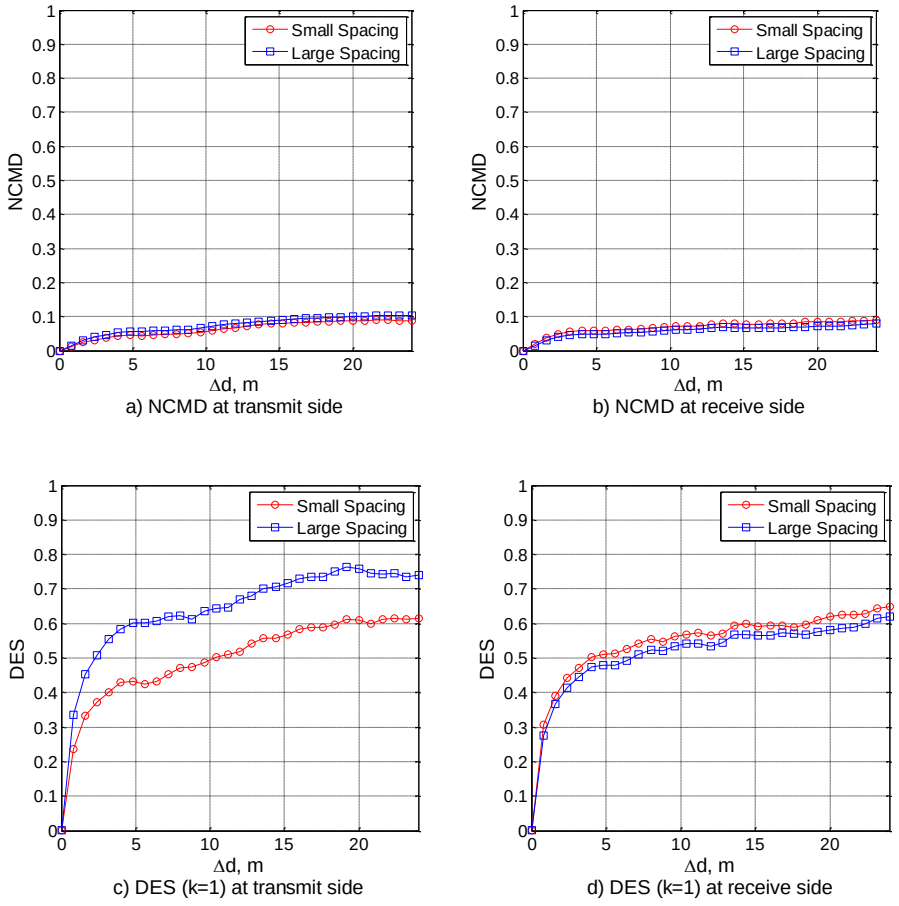

Figure 21: Distance shift versus matrix metric at transmit and receive sides of the small and large antenna spacing at the transmit side for the NLOS route.

Chapter 4
Discussion

4.1 Conclusion

In this thesis, the non-stationarity of MIMO channels was investigated. The main parts of the thesis were to find suitable non-stationarity metrics and to examine these metrics under a measured 4x4 MIMO channel that is applicable to LTE standard.

The non-stationarity of MIMO channel depends strongly on the spatial properties (antenna structures, positions of transmit and receive antennas, etc) in addition to time and frequency. Therefore, it is very important to define a stationarity distance along with stationarity time and bandwidth. For this reason, three MIMO non-stationarity metrics were introduced, namely Correlation Matrix Distance (CMD) proposed by Herdin [**1**], Normalized CMD (NCMD) and Distance between Equidimensional Subspaces (DES). The three metric were applied to the measured channel and compared to each other. The measured channels were divided to LOS, NLOS. Different local stationarity distances were found within these channels.

The CMD metric is based on inner product between two matrices. Under the measured MIMO channel, we found that the CMD does not exceed 0.7 in most cases, similar to the results found in [**1**]. Furthermore, the CMD underestimate the channel non-stationarity compared to DES for beamforming scenario (only one eigenvector is used), similar to the results found in [**14**], but our results show much more difference. This problem become more visible under NLOS channels were the correlation matrix is high rank and noisy. To resolve this, a normalization factor for the CMD was added to ensure that the CMD could achieve its maximum value and the new method was called NCMD.

The normalization factor of the NCMD metric, theoretically, can increase the CMD value up to 100% for 4x4 MIMO system depending on the smallest eigenvalue of the correlation matrix. However, for correlation matrix that is not fully rank (i.e. the smallest eigenvalue is close to zero), the normalization factor will be close to one, as the case for our LOS route. In the NLOS route, we found that the CMD underestimate the non-stationarity by 46% on average compared to NCMD.

The inner product based metrics may not be suitable for some transmission schemes that are based on matrix properties like eigenvectors and eigenvalues. Therefore, we introduce the DES metric that is much more sensitive to the change in these properties. Under the measured channel, we found that these properties are not stationary for NLOS channel environment and fairy stationary for LOS channel.

4.2 Future Work

The field of MIMO non-stationarity has a large potential of improvements. The matrix metrics described so far are not compared yet to any type of transmission schemes. It is very important to relate the non-stationarity metrics to the degradation of the performance of different transmission schemes.

Bibliography

[1] Markus Herdin, "Non-stationary indoor MIMO radio channel," PhD dissertation, Faculty of Electrical Engineering and Information Technology, Vienna University of technology, Vienna, Austria, www.nt.tuwien.ac.at/mobile/theses_finished/PhD_Herdin/paper.pdf.

[2] P. Almers et al., "Survey of channel and radio propagation models for wireless MIMO systems," *EURASIP journal on wireless communication and networking*, vol. 2007.

[3] Ezio Biglieri et al., *MIMO Wireless Communications*. Cambridge University Press, 2007.

[4] G. Matz, "On Non-WSSUS Wireless Fading Channels," *IEE Transactions on Wireless Communications*, vol. 4, September 2005.

[5] H. Hofstetter, W. Utschick I. Viering, "Validity of spatial covariance matrices over time and frequency," in *IEEE GLOBECOM '02 Global Telecommunications Conference* , 2002, pp. 851 - 855 vol.1.

[6] David Tse and Parmod Viswanath, *Fundamentals of Wireless Communications*. Cambridge University Press, 2005.

[7] John G. Proakis and Masoud Salehi, *Digital Communications*, 5th ed., McGraw Hill, 2001.

[8] G. Matz, "Statistical characterization of non-WSSUS," *elektrotechnik und informationstechnik*, pp. 80 -84, 2005.

[9] Gerald Matz, "Doubly Underspread Non-WSSUS Channels: Analysis and estimation of channel statistics," *IEEE Workshop on Signal Processing Advances in Wireless Communications*, pp. 190 - 194 , 2003.

[10] Markus Herdin et al., "Correlation matrix distance, a meaningful measure for evaluation of non-stationary MIMO channels," in *Proceedings IEEE Vehicular Technology Conference (VTC 2005- Spring)*, May 2005.

[11] M. Herdin, W. Weichselberger, J. Wallace, E. Bonek H. Ozcelik, Deficiencies of

'Kronecker' MIMO radio channel model, 2003, *IEEE Electronics Letters*.

[12] Gene H. Golub and Charles F. Van Loan, *Matrix Computations*, 3rd ed., Johns Hopkins Studies in Mathematical Science, 1996.

[13] Adrian Ispas et al., "Analysis of Local Quasi-Stationarity Regions in an Urban Macrocell Scenario," in *IEEE 71st Vehicular Technology*, 2010.

[14] Adrian Ispas et al., "On Non-Stationary Urban Macrocell Channels in a Cooperative Downlink Beamforming Scenario," in *IEEE 72nd Vehicular Technology Conference Fall* , Ottawa, ON , 2010, pp. 1 - 5.

[15] P.A. Bello, "Characterization of Randomly Time-Variant Linear Channels," *IEEE Trans.Commun. Syst.*, vol. CS-11, pp. 360-393, 1963.

[16] David Gesbert et al., "From theory to practice: an overview of MIMO space-time coded wireless systems," *IEEE Journal on Selected Areas in Communications*, vol. 21, no. 3, pp. 281 - 302, Apr 2003.